Friction

Review Article

Research paradigms and scales of asphalt pavement skid resistance evaluation: A review

Zihang Weng[1,2,4], Chenglong Liu[2], Yuchuan Du[2,✉], Zhen Leng[1,✉], Difei Wu[2], Bryan T. Adey[3]

Cite this article: Weng ZH, Liu CL, Du YC, et al. *Friction* 2026, **14**(2): 9441082. https://doi.org/10.26599/FRICT.2025.9441082

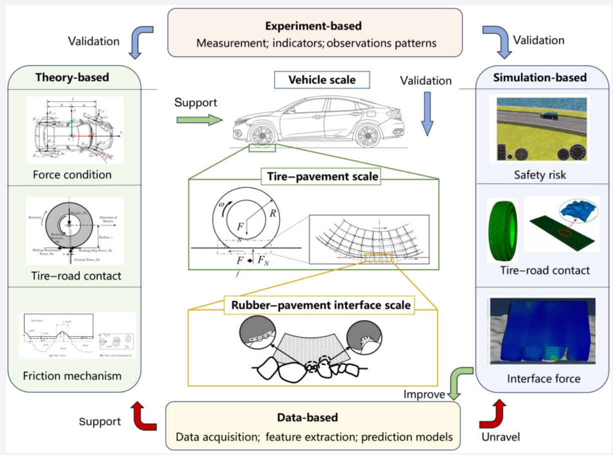

ABSTRACT: Understanding the tire–road friction system is fundamental for evaluating the skid resistance of asphalt pavements. Literature analysis reveals that the trajectory of tire–road friction research aligns with the evolution of scientific research paradigms: experimental science, theoretical science, computational science, and data science. Research in this field can be categorized into three scales: the rubber–pavement scale, the tire–road scale, and the vehicle scale. Experimental observations have yielded numerous patterns and empirical models, which serve as the foundation of this research field. Although numerical measurement devices have been used for decades, the reproducibility and comparability of the results require further improvement. Tire–road friction theory and simulations have been well developed across these three scales, but these scales remain largely independent and unconnected. With the advancement of sensing technology, texture features have been widely exploited and used as inputs for various machine learning models to estimate pavement skid resistance. However, these models are limited in their ability to integrate friction mechanisms, resulting in relatively low interpretability. In summary, the synergistic development of the four research paradigms can promote and advance the understanding and application of tire–road friction mechanisms. This review concludes with a discussion of current challenges and future trends, drawing implications for further research in this field.

KEYWORDS: asphalt pavement; skid resistance evaluation; research paradigms; measurement and modeling

1 Introduction

1.1 Background

The concept of pavement skid resistance pertains to the capacity of road surfaces to provide adequate friction during diverse vehicular operations, including braking, accelerating, and cornering. It is critical for preventing skidding incidents and ensuring driving safety, serving as a significant indicator for road performance evaluation and maintenance decisions. Observations on a London highway by the UK Transport and Road Research Laboratory over four years showed that when pavement skid resistance increased by 50%, the total number of accidents decreased by 45% [1]. Additionally, research by the USA National Transportation Safety Board and Federal Highway Administration [2] indicated that inadequate pavement skid resistance can lead to rear-end collisions, skidding, and rollovers, making it a major cause of driving accidents. Therefore, evaluating pavement skid resistance is of great importance for driving safety.

Research on pavement skid resistance aims to reduce the safety risks associated with vehicle skidding. Therefore, it must be approached from the perspective of the tire–road friction system. Research on tire–road friction systems has been conducted for more than half a century [3]. Early studies focused on enhancing tire–road friction performance by improving the tire's materials and structure. Pavement is often regarded as one influencing variable and is typically treated as a secondary aspect of tire–road research [4]. With the development of the vehicle industry, tire properties such as slip resistance and durability have improved significantly. However, after studying the causes of traffic accidents between 1955 and 1970, Dunlop Tires Company [1] found that simply improving the frictional properties of tires did not reduce the proportion of skidding accidents. Therefore, in the late 20th century, an increasing number of researchers focused on

[1] Department of Civil and Environmental Engineering, The Hong Kong Polytechnic University, Hong Kong 999077, China. [2] The Key Laboratory of Road and Traffic Engineering, Ministry of Education, Tongji University, Shanghai 201804, China. [3] The Institute of Construction and Infrastructure Management, Swiss Federal Institute of Technology (ETH), Zürich 8093, Switzerland. [4] The Hong Kong Polytechnic University Shenzhen Research Institute, Shenzhen 518057, China.

✉ Corresponding authors. E-mail: Y. Du, ycdu@tongji.edu.cn; Z. Leng, zhen.leng@polyu.edu.hk

Received: September 5, 2024; Revised: January 18, 2025; Accepted: February 17, 2025

the skid resistance of the road itself. With the development of sensing technology, high-resolution pavement texture data can be obtained, allowing pavement friction properties to be estimated indirectly and the contribution of pavement texture to the tire–road friction system to be studied. This will help to further investigate the mechanisms of the influence of pavement texture on tire–road friction and thereby propose strategies to improve pavement skid resistance from the perspective of road design and maintenance.

However, tire–road friction is a complex nonlinear issue that is influenced by a multitude of factors. These factors can be categorized into three types: vehicle/tire-related factors, environmental factors, and pavement factors [5]. Vehicle/tire-related factors influence tire–road interactions and friction through operating conditions, physical states, and dynamics of materials. Vehicle-related operating conditions include the slip ratio, load, velocity, etc. Tire-related physical conditions include the tire pattern, tread depth, structure, and inflation pressure [6]. Rubber-related material properties include density, Poisson's ratio, damping ratio, storage modulus, elastic modulus, etc. Environmental factors include medium-related factors, such as water, ice, snow, and contaminants, as well as weather-related factors, such as temperature and humidity. The pavement factors include pavement texture, aggregate properties, asphalt material, additives, etc. Among all the factors, the pavement texture is the most stable variable, while other factors are more volatile [7].

Two key terms, namely, the pavement skid resistance and tire–rubber friction systems, are introduced above. The tire–rubber friction system characterizes the friction forces the tire experiences under specific conditions. Variations in vehicle/tire-related and environmental factors contribute to differences in tire–rubber friction. Based on experimental observations, the pavement skid resistance measurement is essentially a tire–rubber friction system that evaluates representative indicators measured under certain conditions via specific equipment. From the perspective of road researchers, the primary concern is the role that the pavement itself plays within the tire–rubber friction system, which is referred to as the pavement skid resistance. This is an inherent characteristic of the pavement within the tire–road friction system.

Therefore, this study reviews the evaluation of asphalt pavement skid resistance from the perspective of road engineers. The focus of this research does not extend to studies concerning the enhancement of tire/vehicle braking performance or the evolution and enhancement strategies of pavement skid resistance.

After defining the scope of our study, we retrieved 3,041 relevant pieces of papers using "skid resistance & pavement" and "friction & pavement" as search terms in the Web of Science database. We conducted keyword co-occurrence and publication year analyses via VOSviewer [8], and the results are shown in Fig. 1. The proportion of papers published before 2000 is relatively small, so the color bar for this period is compressed in the figure. To ensure the accuracy of the analysis, this study unified similar phrases and excluded unrepresentative terms. Two important findings can be derived from Fig. 1.

(1) The research paradigm has shifted from experiment-based and theory-based paradigms to simulation-based and data-based paradigms. The evolution of tire–road friction research has followed the evolution of scientific research paradigms. The concept of scientific research paradigms was initially introduced by Kuhn [9] in 1962 and refers to the theoretical and methodological foundations of the scientific research operation. There are four generally accepted paradigms: experimental science, theoretical science, computational science, and data science. Early research focused primarily on the experiment-based paradigm, represented by terms such as "measurement", "experimental", "field evaluation", "velocity", and "braking distance", and the theory-based paradigm, represented by terms such as "theoretical". Then, simulation-based paradigm research developed gradually from theoretical research, represented by terms such as "numerical simulation", "hydroplaning", "interaction", and "contact". Currently, the data-based paradigm is the most popular, represented by terms such as "prediction model", "regression model", "deep learning", "feature", and "texture parameter". Generally, data-based research typically includes experimental data. However, this study defines it as research that uses data such as pavement texture to indirectly estimate pavement skid resistance through data modeling.

(2) In terms of research scale, early attention was focused

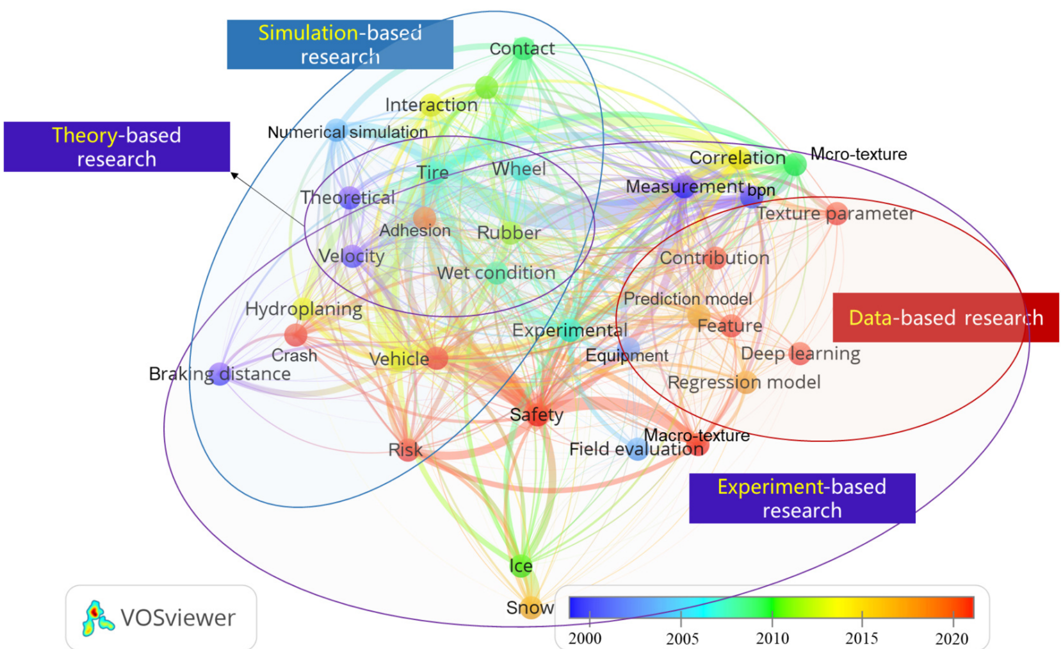

Fig. 1 Keyword co-occurrences in pavement friction studies.

mainly on the tire level, represented by terms such as "tire" and "wheel". The focus shifted to the rubber level in the experiment-based and theory-based research. In recent years, safety risks at the vehicle level, represented by terms such as "vehicle", "risk", "safety", and "crash", have become popular research topics.

On the basis of these observations, we further elaborate on the four research paradigms and three research scales of tire–road friction below.

1.2 Research paradigm evolution of tire–road friction

According to the observations in Fig. 1, the development of research on tire–road friction systems has undergone transitions across four paradigms (Fig. 2). New research paradigms have emerged and become dominant for some time. The depth of the color in Fig. 2 represents the research intensity at the time. The first paradigm, experimental science, laid the foundation for research on the tire–road friction system and thus emerged earliest and dominated the field until the 21st century. Early researchers developed various friction measurement devices and summarized many important patterns through experiments. To better explain the experimental phenomena, theoretical science emerged and developed rapidly from 2000 onwards. Theoretical models have attempted to model tire–road friction under strong assumptions using mathematical and physical models. However, tire–road friction is a complex process involving multiple factors, making it difficult for physical models to fully represent it. With the application of finite element models, simulation science, which simulates the tire–road friction process based on various theories has gradually gained prominence. Nevertheless, simulation models still involve many assumptions and simplifications. With the development of sensing technologies, researchers have attempted to establish a relationship between pavement texture data and skid resistance, and since 2010, data science has become mainstream. The nodes in Fig. 2 represent iconic research examples of different scientific paradigms in the studies of the tire–road friction system.

In the field of tire–road friction system research, the four research paradigms are not entirely independent. Experimental science serves as a benchmark and validation for other paradigms, whereas theoretical science provides the theoretical foundation for simulation science and contributes to mechanistic explanations for experimental science. However, despite simulation science and data science being the main research paradigms for tire–road friction systems, these two paradigms are relatively independent. Data science also struggles to provide data support for revealing the mechanisms of skid resistance theory. Exploring how data science can provide support for revealing the theoretical mechanisms of skid resistance and attempting to bridge the gap between simulation science and data science is an important trend in this field.

1.3 Research scale of tire–road friction

According to the observations in Fig. 1, the research scale of tire–road friction can be categorized into three types: the rubber–pavement interface scale, the tire–road scale, and the vehicle scale, as shown in Fig. 3.

The vehicle scale focuses on braking safety and risk, which is the ultimate goal of tire–road friction studies. The braking risk of a vehicle is influenced mainly by the different forces on tires under different driving scenarios (straight lines, lane changes, curves, downhill, etc.).

However, owing to the different conditions of tires (slip rate, rotational speed, tire properties, etc.) and the uneven distribution of pavement skid resistance, the forces on each tire are not the same. Therefore, the tire-scale research focuses on the force conditions of an individual tire. At the tire–road scale, the tire industry usually adopts the adhesion coefficient to present the overall friction effect between the tire and the pavement, which is defined as the ratio of the total friction force acting on the tire to the vertical load.

Owing to factors such as slip rate, tire pressure, and rubber properties, the contact stress distribution between the tire and the pavement is not uniform [10]. Hence, the rubber–pavement scale focuses on the detailed contact between each hypothetical rectangular block of rubber and the pavement texture. Research at the interface scale decomposes the tire–road system into units, abstracting rubber as idealized block elements. At this scale, the friction properties between the rubber and pavement textures are represented by the friction coefficient. The contact area between the tire and the pavement is divided into several microunits. Each microunit can be envisioned as a block of rubber sliding on the pavement, and the friction coefficient between each rubber microunit and the pavement is defined as the ratio of the tangential force to the normal force acting on the microunit. The

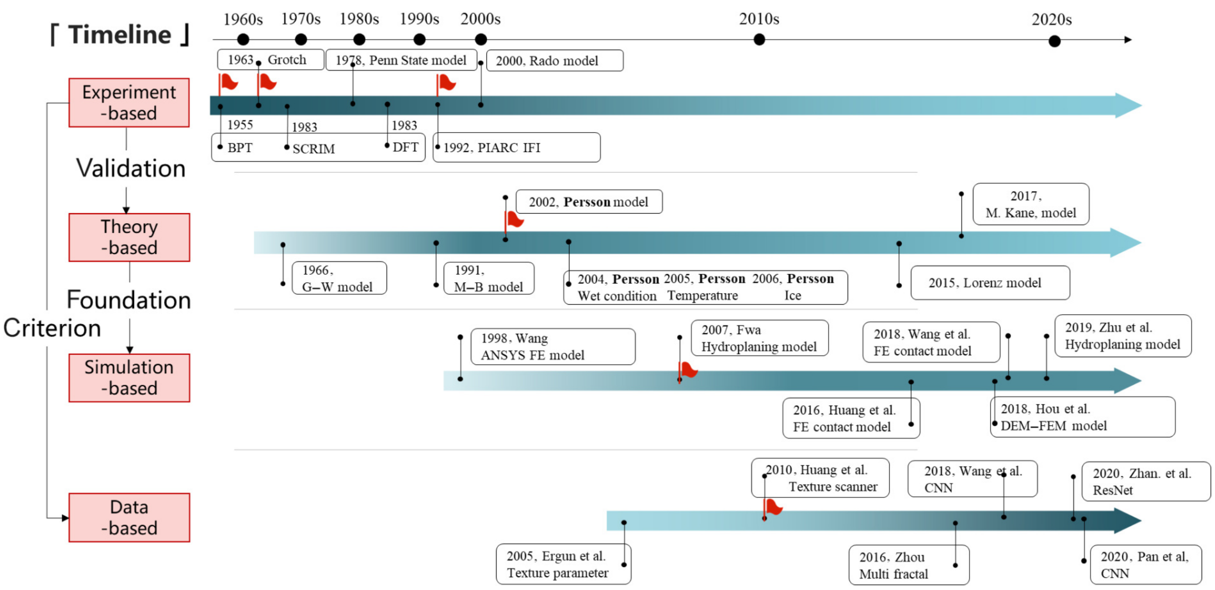

Fig. 2 Development of pavement friction research under different paradigms.

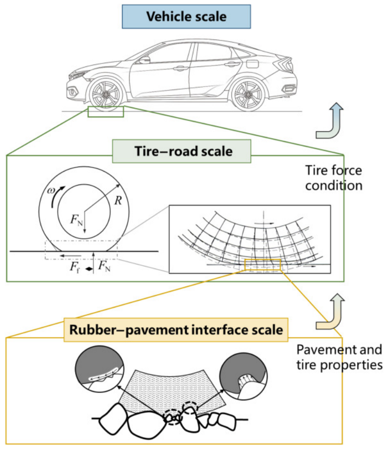

Fig. 3 Three research scales of tire–road friction.

friction coefficient characterizes the frictional properties between microunits of rubber and pavement, reflecting the pavement's skid resistance, which is of greater interest to researchers in the field of road engineering.

This paper presents a causal diagram of the multiple influencing factors in the tire–road friction system (Fig. 4). Pavement factors, environmental factors, and rubber-related material properties affect the friction coefficient at the rubber–pavement interface scale, which indirectly impacts the adhesion coefficient at the tire–road scale. Additionally, the adhesion coefficient is influenced by the environmental factors, tire-related physical conditions (tire pattern, tread depth, structures, inflation pressure, etc.), and vehicle-related operating conditions (slip ratio, velocity, load, etc.). Finally, the adhesion coefficient and vehicle-related operating conditions (velocity, load, etc.) affect slip risks at the vehicle scale. Pavement factors, through their influence on the friction coefficient, subsequently affect the adhesion coefficient and slip risks [11].

This paper outlines a multiscale architecture for tire–road friction research to clarify the representations of different concepts and boundaries, as shown in Fig. 5.

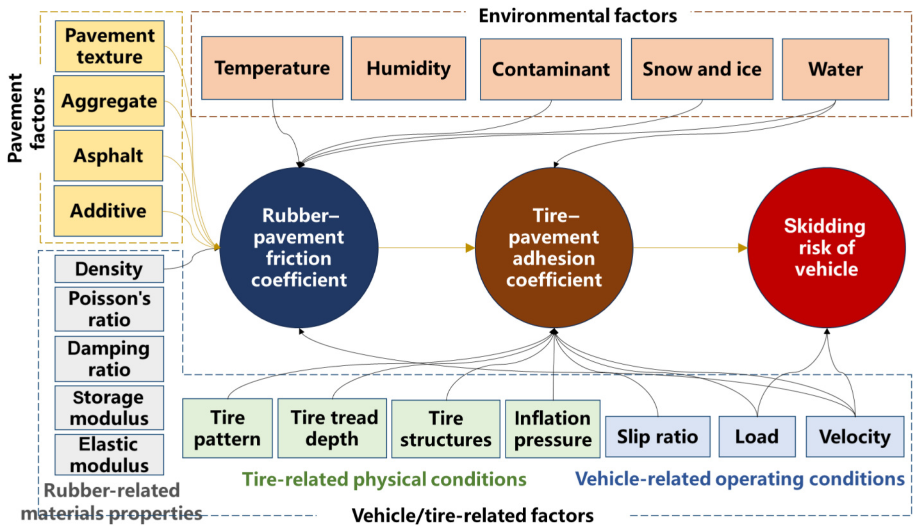

Fig. 4 Causal diagram of multifaceted influencing factors in tire–road friction system.

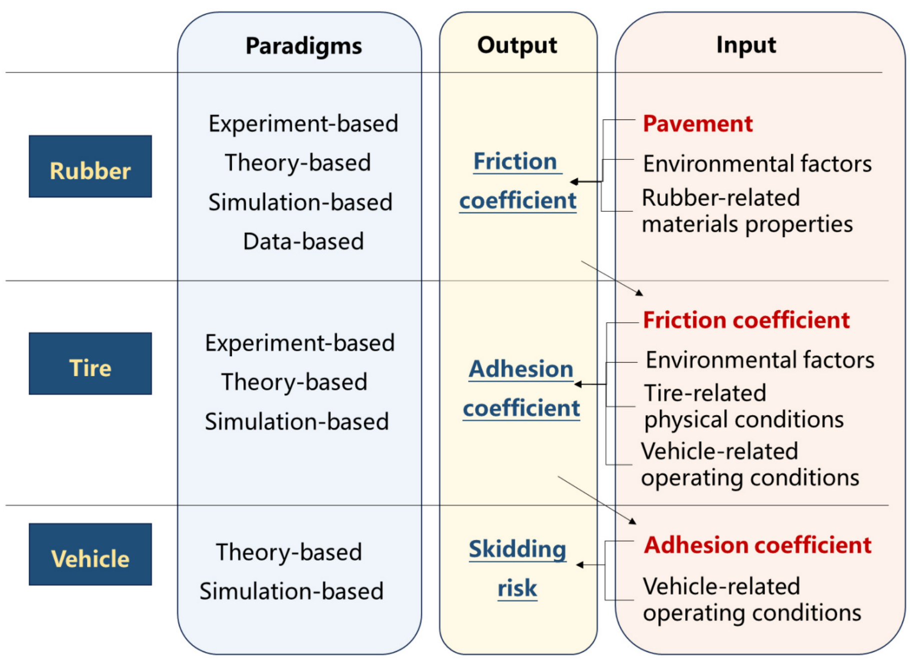

Fig. 5 Multiscale tire–road friction research architecture.

The scale at the interface involves the four paradigms above. At the interface level, pavement skid resistance is an inherent property of the pavement and is represented by tire–road friction in a small sample of the pavement texture.

The research paradigms at the tire–road scale involve mainly theoretical and simulation modeling. The tire scale serves as a key link between pavement properties and vehicle safety. Under uniform tire and environmental conditions, the adhesion coefficient is reflected by the friction coefficient, thereby representing the skid resistance of the pavement.

Research at the vehicle scale focuses primarily on the braking process and uses dynamic theories and simulation modeling to evaluate the skidding risk of the vehicle. At the vehicle scale, the skidding risk is attributed to factors such as road alignment, insufficient pavement friction coefficients, and uneven distributions of these coefficients. Consequently, the pavement skid resistance is the ultimate manifestation of the distribution of pavement textures within the tire–road friction system.

2 Experiment-based research on tire–road friction

2.1 Tire–road friction measurement

Tire–road friction measurements can be categorized into two main approaches: spot-based friction measurements and continuous friction measurements.

2.1.1 Spot-based friction measurement

The British Pendulum Tester (BPT) [12] was developed by the UK's Transport Research Laboratory in 1955. It is a dynamic pendulum impact device used to assess the skid resistance of road surfaces by measuring the frictional work overcome by a rubber slider at the end of a pendulum as it slides across the pavement. The advantages of the BPT lie in its relatively low cost and simple operation. However, it exhibits significant fluctuations in measurement data and cannot measure the friction characteristics at different speeds.

The dynamic friction tester (DFT) [13] was developed in 1983 by a Japanese company. The DFT consists of a lightweight disk with three rubber blocks, which are accelerated to a set speed. The friction coefficient is determined by the amount of rotational kinetic energy lost during the friction process between the disk and the pavement. The DFT can measure the friction coefficient at different speeds, offering advantages such as automated operation, portability, and stable test results.

Laboratory equipment, such as the Wehner–Schulze (WS) machine [14] and the tire–road dynamic friction analyzer (DTFA), is mostly used for experiments. WS, developed in Germany in the 1960s, determines the friction value through three rubber sliding blocks attached to a rotating head and in contact with the sample surface. Laboratory equipment is only suitable for sample tests and cannot be applied to *in situ* measurements, which limits its applicability.

The spot-based friction measurements essentially belong to the rubber–pavement interface scale. The advantages of these methods lie in their intuitive measurement principles and simple operation. However, these measurements cannot fully simulate the various states of the actual tire during the braking process.

2.1.2 Continuous friction measurements

Continuous friction measurements provide a closer approximation of real-world tire conditions and include braking distance measurements, deceleration measurements, sideways force coefficient (SFC) measurements, and longitudinal force coefficient (LFC) measurements [5].

SFC is the ratio of the lateral frictional force generated when the tire is deflected at a specific angle to the vertical load on the test wheel. It represents the lateral friction characteristics of vehicles during side slipping. One of the most typical devices is the sideway-force coefficient routine investigation machine (SCRIM), developed by the UK in 1968. The SCRIM uses a single-wheel deflection method, with the standard test wheel angled at 20° to the direction of travel. The Mu-Meter, on the other hand, is a trailer-mounted device where the towing vehicle provides forward motion. It employs two standard tires symmetrically angled at 15° to the direction of travel.

The LFC is the ratio of the longitudinal frictional force to the vertical load on the test wheel and is measured under conditions where the test wheel aligns with the direction of travel. Depending on the locking state of the test wheel, LFC measurements can be categorized into locked-wheel, fixed-slip ratio, and variable-slip ratio [15]: (1) The locked-wheel measurements involve completely locked wheels with a slip ratio of 100%, including the Skid Resistance Tester-3 (SRT-3) in the UK and the ASTM E-274 Trailer in the USA. (2) The fixed-slip ratio measurements maintain a constant slip ratio for the test wheel, with examples of the Grip Tester (with a slip ratio of 15%) in the UK and the Saab Friction Tester (SFT) in Sweden. (3) The variable-slip ratio measurements allow for adjusting the slip ratio of the test wheel as needed. An example is the ROAR testing system in the USA [16].

Large-scale vehicle or trailer equipment can achieve continuous measurements over a wide range, effectively simulating vehicle braking conditions. However, they are bulky, complex in structure, and expensive. To increase convenience and affordability, low-speed continuous devices such as the micro Grip Tester [17], T2GO [18], and Walking Friction Tester (WFT) [19] have been developed and utilized.

Braking distance measurements are based on the distance a vehicle travels while decelerating from a specific speed to zero. Deceleration measurements are based on the deceleration rate produced by the braking force applied to the vehicle's wheels. These two measurements can reflect the actual motion patterns during vehicle braking and the overall skid resistance characteristics of the pavement. However, it is challenging to standardize test conditions, resulting in lower comparability of results obtained from different test vehicles and scenarios. An increasing number of researchers [20–22] have used the internal parameters of vehicles during the braking process to estimate the friction acting on the vehicle, which is essentially one of the measurement approaches for tire–road friction.

Table 1 lists the characteristics and shortcomings of various measurements. In summary, continuous measurement offers high detection efficiency and better reflects actual vehicle operating conditions, garnering worldwide recognition. However, continuous friction coefficient testing is susceptible to factors such as tire wear, tire pressure, temperature, and driver behavior, making it difficult to control standard conditions and environments. Additionally, these types of equipment typically have large sampling intervals, making it challenging to analyze the correlation between pavement texture and skid resistance performance in detail.

2.2 Tire–road friction evaluation indicators

Tire–road friction evaluation indicators can be classified into three categories: principle-based indicators, equipment-based indicators, and unified indicators.

Table 1 Pavement friction measurements

Categorization		Representative	Indicator	Scale	Image	Advantage	Disadvantage
Continuous	SFC single-wheel	SCRIM (UK)	SFC	Tire		(1) **Applicability**: apply to various on-site scenarios (2) **Range**: broad range for continuous test (3) **Representativeness**: simulates real tire operating conditions	(1) **Applicability**: unsuitable for indoor (2) **Cost**: highly expensive (3) **Sampling**: high sampling intervals (4) **Data**: data variabilities exist due to numerous influencing factors, such as tire wear and environment (5) Prone to being damaged by pavement unevenness, such as potholes and cracks
	SFC dual-wheel	Mu-Meter (UK)	SFC	Tire			
	LFC locked-wheel	SRT-3 (UK) Trailer (US)	SN	Tire			
	LFC fixed-slip ratio	Grip Tester (UK) SFT (SWE) BV-11 (FIN)	SN	Tire			
	LFC variable-slip ratio	ROAR (US) IMAG (FRA) RUNAR (NOR)	SN	Tire			
	Portable hand-held friction coefficient measurement equipment	Micro Grip Tester	μ	Tire		(1) **Applicability**: apply for indoor and on-site scenarios (2) **Range**: broad range for continuous test (3) **Cost**: cost-effective (4) **Sampling**: small sampling intervals	(1) **Representativeness**: simplified tires, not the real tire operating conditions (2) **Data**: data variabilities exist due to influencing factors such as tire wear, tire pressure, temperature, and human operation
		T2GO	μ	Tire			
		WFT	μ	Tire			
	Braking distance measurement		—	Vehicle		(1) **Representativeness**: simulates the actual motion of the braking vehicle (2) **Range**: broad range for continuous test (3) **Cost**: cost-effective	(1) **Applicability**: limited (2) **Sampling**: high sampling intervals (3) **Data**: data variabilities exist when the testing conditions are different
	Deceleration measurement		—	Vehicle			
Spot-based	BPT		BPN	Rubber		(1) **Applicability**: apply for indoor and on-site scenarios (2) **Cost**: low cost (3) **Sampling**: small sampling intervals	(1) **Range**: limited range (2) **Representativeness**: simulate the rubber–pavement friction (3) **Data**: data variabilities exist
	DFT		μ	Rubber	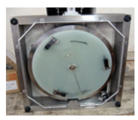		
	TDFA		μ	Tire		(1) **Representativeness**: simulate tire/rubber friction (2) **Data**: stable testing results	(1) **Applicability**: only for indoor tests (2) **Range**: limited range (3) **Cost**: expensive (4) **Sampling**: small sampling intervals
	W/S		μ	Rubber	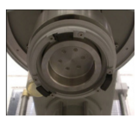		

Note: SWE for Sweden; FIN for Finland; FRA for France; NOR: Norway.

2.2.1 *Principle-based indicators*

Principle-based indicators are defined based on the nature of tire–road friction, such as the friction and adhesion coefficients. In addition, some tests may use the skid number (SN) to represent tire–road friction [23], where the SN is related to the friction coefficient μ: SN = $100 \times \mu$.

2.2.2 *Equipment-based indicators*

Equipment-based indicators are metrics defined specifically for the characteristics of testing equipment, such as the British Pendulum Number (BPN) and SFC. The indicators corresponding to the different equipment are listed in Table 1.

2.2.3 *Unified indicators*

In the 1992 "International Joint Tests" project conducted by the Permanent International Association of Road Congresses (PIARC) organization, 47 types of road skid resistance testing equipment from 16 countries were evaluated [24]. The PIARC

[25] model uses a unified evaluation index named the International Friction Index (IFI), which enables international comparisons. This index aims to convert the results obtained from different types of road skid resistance testing equipment at various slip speeds into a standardized metric. All the measured values are adjusted to the friction coefficients at a skidding speed of 60 km/h, known as F_{60}. The estimated friction coefficient at speed S is calculated via Eqs. (1)–(3):

$$F(S) = F_{60} \times \mathrm{e}^{(S-60)/S_{\mathrm{p}}} \tag{1}$$

$$F_{60} = A + B \times \mathrm{FR}_S \times \mathrm{e}^{(S-60)/S_{\mathrm{p}}} + C \times T_{\mathrm{x}} \tag{2}$$

$$S_{\mathrm{p}} = a + bT_{\mathrm{x}} \tag{3}$$

where T_x represents the pavement texture depth; a and b are calibration parameters for the pavement texture; A, B, and C are calibration parameters for the friction testing device; S represents the skidding speed; FR_S refers to the measured friction coefficient under the skidding speed S.

In 2018, Quiros et al. [26] evaluated several methods for converting to the IFI and proposed an alternative approach. However, research has shown that unified indicators such as IFI do not apply to all devices [27]. Furthermore, the consideration of pavement texture in the models is limited to the texture depth indicator and cannot finely characterize the influence of pavement texture on tire–road friction.

2.3 Patterns in tire–road friction research based on experimental observations

Based on the measurement equipment and evaluation indicators, researchers have observed numerous patterns related to influencing factors through experiments.

2.3.1 Vehicle-related factors

In 1934, Moyer [28] reported through experiments that the pavement friction coefficient was negatively correlated with the slip velocity. In 1978, Leu and Henry [29] proposed the Penn State model, which describes the mathematical relationships among indicators, texture characteristic parameters, and slip velocity. However, it is not feasible to measure the value of slip speed as 0 under normal conditions, limiting the application of the Penn State model. With the emergence of various types of equipment, it has become difficult to unify evaluation results. In 2000, Hall et al. [2] proposed the classic Rado model, which delineates the relationship between the friction coefficient and slip speed.

2.3.2 Tire-related factors

With respect to tire-related factors, the primary focus is on tire–road contact characteristics. Researchers have summarized patterns through experimental methods such as pressure plates, pressure sensors, pressure-sensitive films, and light absorption.

In 1986, Pillai and Fielding-Russell [30] conducted experiments on the tire footprint area and proposed empirical formulas based on tire deformation and sidewall size parameters. In the same year, Marshek et al. [31] conducted pressure distribution tests on truck tires using pressure-sensitive films. In 2003, Koehne et al. [32] explored the shear and vertical stress distributions of tread blocks in the contact area of slick tires, longitudinally patterned tires, laterally patterned tires, and tires with fine grooves through experiments. Since 2014, Zhang et al. [33] have attempted to conduct a series of experimental studies on the pressure distribution of the tire–road interface contact using a pressure film measurement system. Wang et al. [34] verified the relationship between the contact pressure and penetration depth by testing the pressure distribution of tire–road contacts. In 2022, Yun et al. [35] designed a mechanical loading device to test the contact conditions between rubber and three-dimensional (3D)-printed pavement models.

However, although tire–road contact methods based on experimental measurements allow direct observation, the high cost of experiments and the limited applicability and generalization of experimental contact results often restrict their widespread use.

2.3.3 Pavement texture

Researchers have investigated the relationships between texture parameters and skid resistance indicators for pavement textures to construct empirical prediction models.

Meegoda [36] conducted experiments using DFT and a circular texture meter (CTM) and established a linear empirical formula for the friction coefficient based on mean profile depth (MPD). Ergun et al. [37] built a multivariate empirical formula based on texture structural parameters. Wu et al. [38] established a nonlinear prediction model for the friction coefficient F_{60} based on MPD and DFN20. In 2017, Wasilewska et al. [39] observed the macrotextures and friction coefficients of newly constructed roads using CTM and DFT. They found that in the initial stage of road use, when the initial friction coefficient was relatively low, the macrotexture did not change significantly.

These methods rely solely on experimental observations to construct empirical models of the relationship between different texture parameters and skid resistance indicators, which are representative but limited in their ability to delve into the coupling frictional relationship between rubber and pavement texture.

2.3.4 Water film

Researchers have also conducted a series of experimental studies on the influence of water films, with a primary focus on tire hydroplaning.

They established empirical formulas for critical hydroplaning speed through tire hydroplaning tests, including the National Aeronautics and Space Administration (NASA) [40] formula and Gallaway [41] formula. The NASA formula proposes the critical hydroplaning speed for aircraft tires based on experiments, which is a classic formula but does not consider factors such as pavement characteristics and water film thickness. The Gallaway formula describes the mathematical relationship between the critical hydroplaning speed of tire and factors such as tire pressure, tread depth, water film thickness, and pavement texture. Additionally, Wray and Ehrlich [41] experimentally studied the effects of tread depth, pavement texture, tire pressure, load, and tire deformation on tire hydroplaning. Wies et al. [42] analyzed the effects of tread direction, position, and area on tire hydroplaning. Do et al. [43] used DFT to test the effect of water film thickness on tire–road friction and defined the critical water depth between boundary lubrication zones and mixed lubrication zones on the basis of the Stribeck curve.

However, tire hydroplaning tests have high requirements for test sites and equipment, as well as high experimental costs. More research has focused on tire hydroplaning, but there is still a lack of research on hydroplaning safety assessments that consider the pavement texture.

In summary, experimental observations can yield numerous patterns and empirical models. However, such research on pavement texture contributes only to the understanding of macro parameters such as texture depth. Research is a process from phenomena to essence, and on the basis of experimental conclusions, it is necessary to explore the intrinsic mechanisms of pavement skid resistance. Therefore, the research focus has gradually shifted toward theoretical science.

3 Theory-based research on tire–road friction

3.1 Friction mechanism at rubber–pavement interface scale

Owing to the complexity of the tire–road friction system, most theoretical models simplify the tire as a rubber slider for analysis at the interface scale. In 1963, Grosch [44] revealed that the friction between rubber and pavement primarily comprises adhesive and hysteresis components (Fig. 6). The coefficient of pavement friction can be expressed as Eq. (4):

$$\mu = \mu_{\mathrm{Hys}} + \mu_{\mathrm{Adh}} \tag{4}$$

where μ_{Hys} represents the hysteresis friction coefficient and the adhesive friction coefficient.

The adhesive component [45] is the shear force generated at the interface between the rubber and the pavement, which mainly includes intermolecular van der Waals forces, the adhesion between the tire and the pavement, and the microcutting action of the pavement asperities (Fig. 7). Its magnitude is related to the roughness of the contact interface and is influenced primarily by the pavement microtexture. The essence of the hysteresis component is related to the energy dissipation associated with the deformation of the tire during sliding [46].

Furthermore, Grosch investigated the influence of velocity on the rubber–pavement friction force components and reached important conclusions: (1) The hysteresis component gradually becomes dominant with increasing sliding speed of the rubber [47]; (2) at low speeds, the adhesive component dominates. In 1987, the PIARC [48] further verified Grosch's conclusion, indicating that hysteresis friction accounted for 90% of the friction force at a speed of 90 km/h on wet pavements.

The classical Amontons–Coulomb law does not apply to rubber–pavement friction, and researchers have proposed several theoretical and semi-theoretical models to describe the friction process.

The brush model [49], proposed in 1958, is a general model physically derived from variants of the brush model. In this model, it is assumed that the surface area that is in contact with the road can be modeled as infinitesimal bristles. The contact patch area is partitioned into two regions: adhesion and sliding. The LuGre model, introduced by de Canudas et al. [50] in 1995, is a velocity-dependent model designed to describe the hysteresis loop and the displacement preceding sliding. Do and Delanne [51] presented a model for the speed dependency of friction on the basis of the knowledge of its variation with speed described by the Stribeck curve.

In 2001, Persson [52] characterized pavement texture features on the basis of power spectral density, fractal dimension, and waviness cutoff frequency. The Persson model was established to provide a detailed characterization of rubber energy dissipation in tire–road friction processes. This work serves as the theoretical basis for subsequent research on rubber–pavement hysteresis friction coefficient calculations. However, this model neglects the adhesive component and calculates only the hysteresis component. In subsequent studies, Persson considered the randomness and anisotropic characteristics of pavement as well as the influence of the lubrication layer in the contact model [53]. Additionally, Persson further accounted for thin water films [54], temperature [55], and ice [56] in rubber–pavement friction. Kluppel and Heinrich [57] also proposed a model similar to the Persson theory, with the difference of replacing the wavelengths of the pavement in the Persson model with frequencies.

Persson's theory has a great impact on tire–road friction research, with many researchers validating it through experimental measurements. Tanaka et al. [58] in Japan and Ueckermann et al. [59] in Germany conducted indoor and outdoor experiments to verify the correlation between Persson's results and the measured values, which showed good agreement. In 2015, Motamedi [60] combined macro- and microscales with Persson theory and validated the model's accuracy through indoor experiments. By incorporating Persson's friction theory, Tan et al. [61] established and verified a mechanical model for the skid resistance of ice and snow-covered road surfaces via an improved DFT. Another group of researchers has delved into and expanded theoretical models on the basis of Persson's theory. Lorenz et al. [62] proposed a semi-empirical adhesive component model to further refine the theoretical model of friction coefficients. Xu et al. [63] introduced the theory of molecular surface free energy to supplement the calculation method for the adhesive friction coefficient. In addition, Ciavarella [64] simplified Persson's multiscale friction theory by considering the viscoelastic losses of rubber. Alhasan et al. [65] utilized Persson's theory to establish a mechanical computational model for a pendulum tester. In 2023, Persson [66] calculated the probability distribution of surface stress in response to a uniform external tensile stress with the displacement vector field parallel to the rough surface. Numerical simulation results were presented for the stress distribution and revealed that in a typical case, the maximum local tensile stress may be more than 10 times greater than the applied stress. In 2015, Kane and Cerezo [67] simulated the rubber–pavement friction behavior of DFT and proposed a model for calculating the friction hysteresis component. In 2019, Kane et al. [68] considered the viscoelasticity of tire rubber, the pavement texture, and the

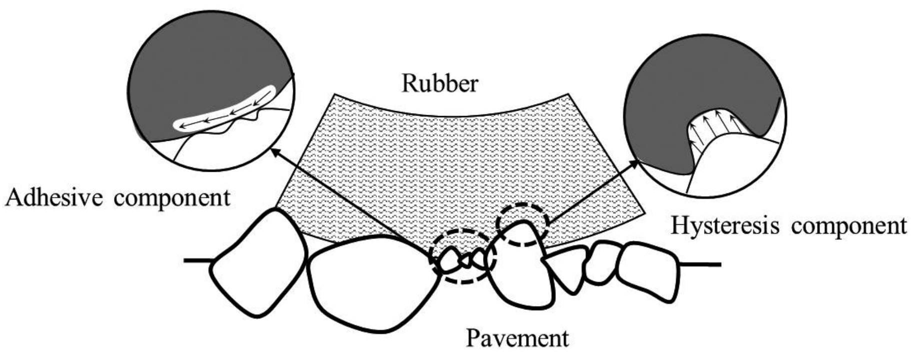

Fig. 6 Composition of tire–road friction.

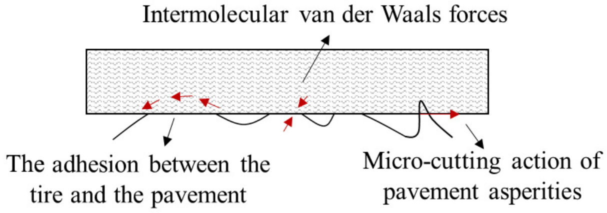

Fig. 7 Composition of adhesive friction.

water layer effect in the calculation of tire–road hysteresis friction. Löwer et al. [69] proposed a model to describe the contact characteristics of tire–water–pavement, considering the water squeezing out between a viscoelastic rubber block and pavement. Some classic theoretical and semi-theoretical models at the rubber–pavement scale are summarized in Table 2.

In conclusion, most theoretical and semi-theoretical models lack sufficient consideration for integrating high-resolution 3D pavement texture features. A future research trend that theoretical studies need to focus on is how to enhance the characterization ability of theoretical models for actual tire–road friction via 3D pavement data.

3.2 Theoretical and semi-theoretical model at tire–road scale

The earliest research on friction theory at the tire–road scale focused mainly on tires. Since the 1930s, researchers have continuously enriched tire dynamic models, evolving from linear to nonlinear, from steady-state to nonsteady-state, and have proposed theoretical models, semi-theoretical models, adaptive models, etc. Additionally, models based on tire dynamics parameters such as the slip ratio and slip velocity have also been proposed. The Dugoff tire model [70], proposed in 1969, is a velocity-independent tire model. This approach considers the coupled relationship between the longitudinal and lateral forces. Gim and Nikravesh [71] established a dynamic equation of tire–road contact on the basis of the steady-state UA tire model. On the basis of the classical magic formula model [72], the brush model, and experimental data, Guo et al. [73] proposed the semi-empirical and semi-theoretical tire model UniTire.

However, the models above have a limited ability to consider the pavement texture. Given the complexity of tire–road friction, researchers initially focused on theoretical tire–road contact models. As early as 1882, Hertz [74] developed a nonadhesive contact model in which surface contact was assumed to be elastic and highlighted a nonlinear relationship between the contact stress and applied pressure, which was influenced by the material's elastic modulus and Poisson's ratio. In 1957, Archard [75] proposed an approximation of a linear relationship between the real contact area and applied pressure on the basis of multiple contact assumptions. In 1966, the Greenwood and Williamson (G–W) model [76] incorporated the texture characteristics of the contact surface, assuming that the texture asperities are semicircular. In 1977, the Sayles and Thomas (S–T) model [77] accounted for the unstable stochastic nature of the pavement texture, considering an uneven distribution of texture asperities. In 1991, Majumdar and Bhushan [78] introduced the M–B contact model based on fractal geometry, simplifying the contact of rough surfaces as the interaction between an equivalent rough surface and an ideal rigid smooth surface. In 2003, Canudas et al. [79] derived a tire–road contact model capable of capturing the transient behavior of friction between braking and acceleration. However, the contact models overlook the interaction between different contact regions. In 2012, Pinnington [80] presented an algebraic model of a general surface to cover the full wavelength range for the road–tire interaction. A truncated Fourier series describes the particle shapes and the envelope of particle peaks as a truncated Weierstrass–Mandelbrot function. In 2022, Kane and Edmondson [81] proposed a physical model at the tire scale that considers parameters related to the tire, pavement, contaminants, and contact conditions. However, their model relatively simplistically considers the influence of the pavement texture and estimates the friction coefficient solely through multiscale fractal features of the pavement texture.

The models at the tire–road scale involve numerous simplifications and assumptions, but provide a theoretical foundation for tire simulation modeling.

3.3 Theoretical model at vehicle scale

At the vehicle scale, researchers have considered the overall friction acting on the wheels as a resultant force and focused on the safety risks posed by this friction on the vehicle. In 1998, Lenasi et al. [82] dealt with the behavior of a vehicle in the laterally stable and unstable areas caused by friction during braking via a vehicle's theoretical model, as shown in Fig. 8(a). Through force analysis, it was shown that vehicle stability might be jeopardized or completely lost when one or more wheels exceed the friction limit and that vehicle lateral instability always results from torque imbalance.

To meet the demands of subsequent vehicle simulations, the complexity of the vehicle's theoretical model has gradually increased. Zhang and Göhlich [20] selected a vehicle model with greater dynamic complexity (Fig. 8(b)) as the basis of the simulation, considering longitudinal and lateral friction, turning torque, and wheel turning angular velocity.

Table 2 Classic theoretical and semi-theoretical models at rubber–pavement scale

Model	Published year	Type	Assumption and description
Brush	1958	Physical based	(a) The friction is assumed to be constant (b) The effect of carcass deformation is neglected (c) The elements are assumed to be linearly elastic
LuGre	1995	Dynamic tire-based	The surfaces are assumed to be in contact through elastic bristles
Kluppel	2000	Fractal theory-based	Use the time–frequency domain
Persson	2002	Fractal theory-based	(a) Neglects the adhesive component (b) The pavement texture was regarded as a self-similar surface
Minh	2004	Stribeck curve-based	Assume that the calculation of friction at any speed would need an estimate of friction at a very low speed
Lorenz	2015	Semi-empirical and semi-theoretical	Assume that the adhesive component is primarily constituted by the shear stress on the contact surface
Löwer	2020	Physical based	Consider the water squeezing out between a viscoelastic rubber block and pavement

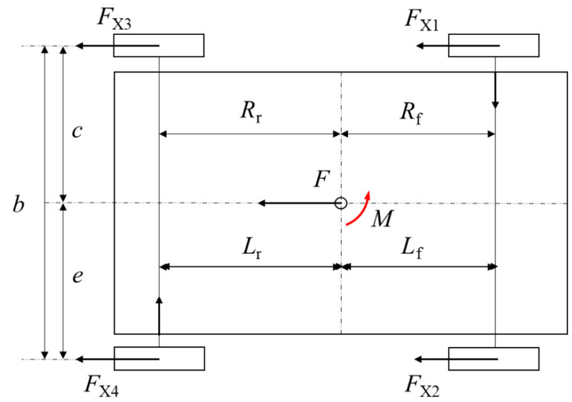

(a) Simple vehicle theoretical model

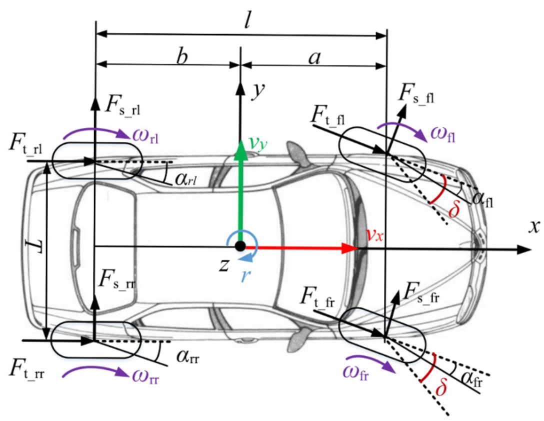

(b) A vehicle model with more dynamic complexity

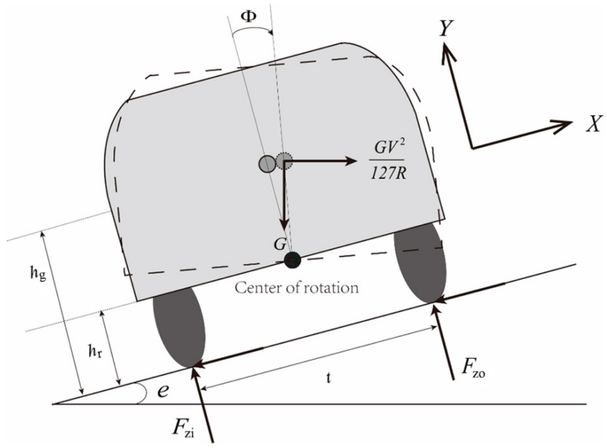

(c) Cross-sectional vehicle theoretical model

Fig. 8 Vehicle theoretical model. Reproduced with permission from Ref. [82] for (a), © Taylor & Francis 1998; from Ref. [20] for (b), © the authors 2017; from Ref. [83] for (c), © the authors 2022.

Compared with straight roads, vehicles have relatively larger turning angles and an increased risk of skidding on curved roads. Xu et al. [83] developed an integrated risk assessment framework to evaluate safety on horizontal curves (Fig. 8(c)), considering the lateral distributions and evolution of the friction coefficient under different traffic characteristics.

The vehicle scale involves the combined effects of multiple systems, such as suspensions, tires, and engines. Some parameters in the vehicle theoretical model are difficult to obtain or assess. Therefore, the theoretical model of the vehicle is usually regarded as the theoretical basis for vehicle simulation research, which will be introduced in Section 4.3.

Currently, research on theoretical models of tire–road friction systems has developed relatively early, but progress has slowed in recent years. This is largely due to the highly nonlinear issues involved in studying tire–road friction behavior, such as the viscoelastic characterization of tires and contact properties. Theoretical models often involve excessive simplifications, and empirical formulas are limited by various factors. Therefore, simulation has become a crucial paradigm for analyzing tire–road contact friction.

4 Simulation-based research on tire–road friction

Large-scale field experiments require significant labor and resources, and there are inherent safety risks, especially under high-speed conditions. Additionally, theoretical models struggle to further describe complex, multi-factor coupled mechanical processes. Since the 1970s, with the rapid development of nonlinear finite element theory and computational software, researchers have increasingly used simulation methods to study tire–road friction at three scales: rubber, tire, and vehicle, as shown in Fig. 9.

4.1 Simulation at rubber–pavement interface scale

Rubber–pavement friction simulations primarily consider the shear action between rubber and the pavement texture, so researchers typically simplify the tire to a rubber block. In 2018, Hou et al. [84] integrated a multiscale discrete element and finite element method to simulate the rubber–pavement friction process with relatively low computational cost. In 2019, Peng et al. [85] established a friction model between rubber blocks and pavement textures on the basis of finite element analysis and utilized a binary search inversion method to determine the interface friction parameters. Guo et al. [86] used molecular dynamics simulations to study the confined shear process between rubber and textures. The results revealed that the simulated friction coefficient increased and then decreased with increasing velocity, which was attributed to changes in the average longitudinal stress during the friction process. Similarly, in 2023, Xiao and Cheng [87] employed molecular dynamics to establish a contact model, estimating the rubber–pavement friction force under wet conditions and comparing it with results obtained via a pendulum method.

Rubber–pavement friction simulations at the rubber–pavement interface scale can reveal the mechanical behavior of rubber in contact with the pavement texture at a microscopic level. However, current research often inadequately considers detailed 3D pavement textures, with most studies simplifying the pavement texture and overlooking issues such as the compression and stress distribution caused by the texture of the pavement on the rubber. Löwer et al. [88] proposed a model of a single-tread block on a rough road surface with the influence of the fluid represented by a physically meaningful friction law. The model is validated with the results of tire wet-braking tests on an internal drum test rig. The model can map the interaction between the tire tread, rough road surface, and fluid film, and the simulation results are in good agreement with the measurement results.

4.2 Simulation at tire–road scale

Simulation studies at the tire–road scale have focused mainly on tire–road contact/friction and tire hydroplaning.

4.2.1 *Tire–road contact and friction*

The tire–road contact process is a complex, multi-factor coupled

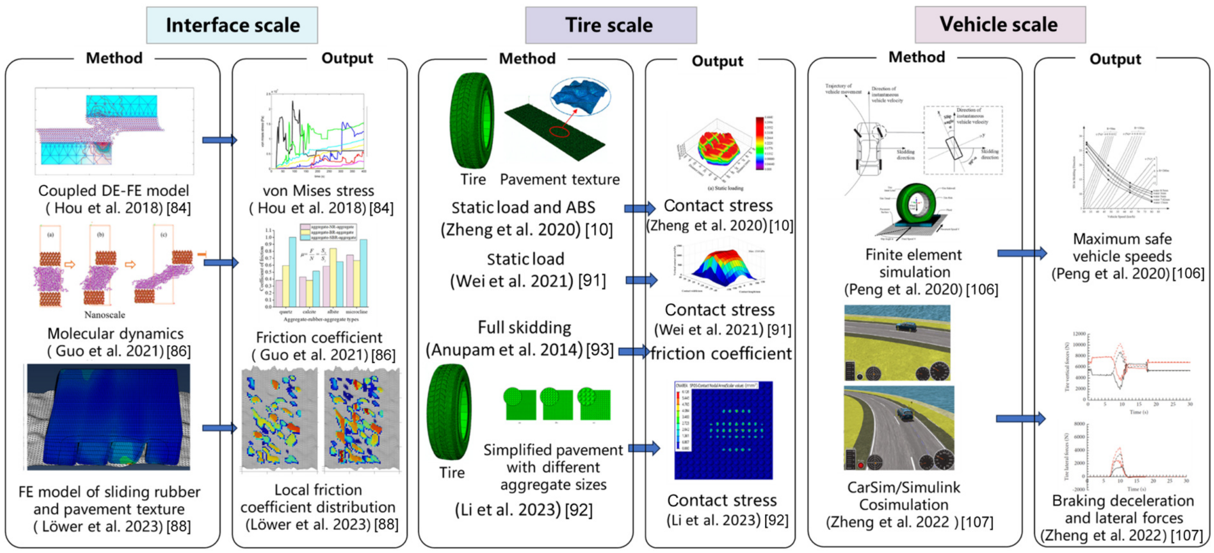

Fig. 9 Methods and outputs of simulation-based research on tire–road friction. Reproduced with permission from Ref. [84], © Informa UK Limited 2018; from Ref. [86], © Elsevier Ltd. 2021; from Ref. [88], © the authors 2021; from Ref. [10], © Informa UK Limited 2020; from Ref. [91], © Informa UK Limited 2021; from Ref. [93], © National Academy of Sciences 2014; from Ref. [92], © the authors 2023; from Ref. [106], © Informa UK Limited 2020; from Ref. [107], © the authors 2022.

process, and the advantage of simulation modeling lies in its ability to analyze multiple variables one by one to explore the extent of their impact on the system.

Tielking and Roberts [89] utilized ILLI-PAVE to compute large deformations in tire–road contacts. Burke and Olatunbosun [90] conducted gap element simulations on the MSC/NASTRAN platform to obtain tire–road contact imprints under specific conditions. Zheng et al. [10] established a 3D contact model of tires and pavement via the finite element method to investigate the effects of tire inflation pressure and load. They simulated different tire states (static load and antilock braking system states) and reported that under the antilock braking system state, the average contact pressure increased by 8.4%, whereas the contact area decreased by 7.7%. Wei et al. [91] used finite element models to simulate the stress distribution during tire contact with road textures and concluded that all the tested pavement types led to stress concentrations. Li et al. [92] analyzed simplified road surfaces with rough aggregates via Abaqus and different diameters of hemispherical shell models to simulate the contact between a tire and a road surface.

Compared with contact friction, tire–road friction is more complex and hence less researched. Anupam et al. [93] utilized finite element methods to construct a simulation model for rolling pneumatic tires and investigated the influence of temperature on cornering friction [94]. The results indicated that higher road, ambient, and air temperatures lead to a decrease in the hysteresis friction component.

The existing numerical simulation studies have focused mainly on tire–road contact, especially under static loading conditions, with only a few considering the anti-lock braking system state. Furthermore, the results regarding the contact area and pressure are only applicable to specific samples and lack sufficient consideration for the generalizability and transferability of the research.

4.2.2 Tire hydroplaning

Under wet conditions, tire–road contact and friction involve fluid mechanics due to water expulsion and hydroplaning effects, increasing the complexity of research. Among these, hydroplaning has received the most attention. Hydroplaning is the phenomenon where a tire loses contact with the road surface due to the lifting action of water while traveling at high speeds.

Ong and Fwa [95] proposed a numerical simulation model for simulating tire hydroplaning in 2007, which demonstrated that the NASA equation is a general solution and is applicable only to specific tire contact conditions. Subsequently, the hydroplaning model was used to analyze the braking distances of vehicles under different depths of ruts in wet conditions [96]. Building upon this, Ding and Wang [97] proposed a method for calculating speed limits on the basis of the required safe braking distance. Choi et al. [98] considered the lubricating effect of water and analyzed the influence of 3D tire tread patterns on the contact pressure and dynamic water pressure. Research has shown that the fluid pressure during hydroplaning is proportional to the square of the velocity. Ding and Wang [97] established a tire–water–pavement model to predict the hydroplaning speed under different pavement types, rainfall intensities, and rutting depths with an antilock braking system. Zhu et al. [99] established a finite element model of tire–water–pavement in Abaqus and studied the influence of water film thickness and tire speed on tires. Zhu et al. [100] studied the hydroplaning of aircraft tires and established a finite element model to analyze the effects of different factors (such as speed, wear ratio, runway type, water film depth, and slip ratio) on runway skid resistance by considering real runway surfaces and different water film depths. Luo et al. [101] developed a tire–water–pavement finite element model to evaluate the degradation of the skid resistance of different pavements and the coupling effects of the texture evolution and factors of the slip ratio, slip angle, velocity, and water film on the braking-cornering characteristics of the tire. Fan et al. [102] realized a local fine fluid–structure coupling simulation of tire–water–pavement based on the Euler–Lagrange algorithm. The study revealed that the reduction rates of the friction coefficient under 5 and 15-mm water films were 34% and 65%, respectively, when the vehicle speed was 80 km/h.

Currently, numerical simulation research on tire hydroplaning has made significant strides. However, further refinement is needed, particularly in areas such as the distribution of water film thickness and pavement texture.

4.3 Simulation model at vehicle scale

Simulation at the vehicle scale is primarily aimed at assessing the braking risk of the vehicle–road system, including modules such as vehicle models, tire models, suspension models, controllers, engines, and pavements. The lateral stability of a vehicle under various driving conditions on wet pavement has been the research focus [103].

Liu et al. [104] calculated the braking distances in a vehicle model using the tire hydrodynamic forces obtained mechanically from a hydroplaning model with different water film thicknesses. The results show that both longitudinal braking distances and lateral slip distances should be considered in the evaluation of vehicle braking performance.

You and Sun [105] established a driver/vehicle/road closed loop dynamic simulation model via Matlab/Simulink for reliability analysis of vehicle stability on a combined horizontal and vertical curve. Pavement friction and vehicle operating speed were the important inputs. The results show that the probability of skidding calculated by the vehicle dynamic simulation is greater than that by the point-mass model, and the probability of failure decreases with increasing superelevation and increases with increasing road slope.

Peng et al. [106] determined the maximum safe driving speed for a vehicle on a horizontal pavement curve through a tire–road finite element simulation model under different water film depth conditions.

Zheng et al. [107] built a braking model of autonomous vehicles in Simulink and analyzed the braking performance on curved sections with CarSim/Simulink co-simulation. The results indicate that both the maximum lateral offset distances and the maximum lateral forces of the tires decrease as the curve radius gradually increases under different road conditions. Additionally, there is a relatively uniform vertical force distribution of the tire when the curve radius is no less than 100 m, and the limit speed of the vehicle varies parabolically with increasing curve radius.

Zhao et al. [108] calculated the probability of hydroplaning based on the water film thickness distribution and the probabilistic model of speed and wheel track, and the hydroplaning risk was set to five levels according to the probability.

Currently, simulation studies at the vehicle scale are scarce, with considerations of operating conditions and scenarios being relatively limited. Integration with the spatial distribution of pavement skid resistance performance is insufficient, leaving ample room for further exploration.

In summary, numerical computation and simulation studies of tire–road friction are rapidly advancing, but they are currently focused primarily on the tire scale. There is relatively less research on the rubber–pavement scale and the vehicle scale. There is also a lack of exploration regarding the conversion of tires to rubber scales. Additionally, numerical computation and simulation methods face challenges in analyzing overly intricate microtextures of road surfaces. Therefore, the contribution of microtextures currently relies mainly on the combination of experimental testing and data collection, which also drives the development of paradigms for data-based research on tire–road friction.

5 Data-based research on tire–road friction

Before the 21st century, owing to limitations in data acquisition capabilities, the understanding of pavement texture characteristics was previously limited to the indicator of texture depth. With the development of 3D pavement texture data acquisition technologies, the data quality, resolution, and range have significantly improved, making it possible to extract finer texture features. The increased volume of data has also spurred research into data-driven models based on machine learning. The research was conducted on three levels: data acquisition, feature extraction, and prediction models.

5.1 Data acquisition

The methods for data acquisition for pavement textures can be classified into indirect and direct methods.

Indirect methods, such as the sand patch test and the outflow meter test, focus primarily on detecting the mean texture depth (MTD), with the most commonly used methods [109, 110]. Both are based on volumetric principles and offer intuitive indicators. However, indirect methods suffer from low efficiency, accuracy, and reproducibility. This indicator cannot comprehensively reflect various characteristics of the pavement texture.

Direct methods include contact probes, image-based methods, and laser scanners. In addition, researchers have explored various sensing methods, such as laser interference fringe [111], laser radar [112], and hyperspectral remote sensing [113]. However, these methods are still in the research stages and have not been widely applied.

5.1.1 Probe test

The contact probe test method utilizes the displacement of miniature probes sliding on the road surface to obtain pavement profiles. German researchers developed the T8000 contact probe [114], which achieved an accuracy of up to 0.1 μm. Contact probes have advantages such as testing stability and high measurement accuracy, but are limited to laboratory measurements. Additionally, the testing range is limited, and the use of high-hardness probes may damage the pavement texture. Noncontact probe tests trace and record the light behavior, achieving nanoscale sensing in a nondestructive way. However, the test is very sensitive to surface qualities and thus has high data variability and low accuracy [12].

5.1.2 Image-based methods

Image-based methods, which use cameras as sensors to capture two-dimensional (2D) or 3D information on the road surface, can be classified into three types: monocular, binocular, and multi-ocular stereo reconstructions.

Monocular vision stereo reconstruction estimates the 3D structure of the pavement from a single image, deriving depth information from 2D features such as contrast, contours, and complexity of the image [115]. In the late 1960s, the British Road Research Laboratory began to estimate texture characteristics via 2D images. Since the beginning of the 21st century, Wang et al. have utilized images to evaluate pavement texture depth. Nejad et al. [116] proposed an image-based road skid resistance estimation system. Based on 2D images, Weng et al. [117] and Du et al. [118] used neural networks to predict pavement texture depth and skid resistance, respectively. However, the texture characteristics estimated from 2D images are limited, and the accuracy remains uncertain.

Binocular vision stereo reconstruction converts binocular disparity information into depth information, which is most in line with human visual mechanisms. The core is feature matching, which directly affects the accuracy of the reconstruction results.

While multiocular stereo reconstruction involves more sources of information, it also poses greater challenges in feature matching. Chen et al. [119] established a system for reconstructing

3D pavement textures via three-camera close-range photogrammetry technology. Sun and Wang [120] improved photometric stereo techniques for higher accuracy using low-rank matrix recovery methods.

Both binocular and multi-ocular stereo reconstructions have lower costs, but their detection accuracy is still not as high as that of laser-based equipment. They also require specific camera setups and are more suitable for laboratory settings; hence, they have not been widely adopted in engineering applications.

5.1.3 Laser scanners

The laser scanners are based on the triangulation principle and can be divided into 2D laser profilers and 3D laser scanners. Two-dimensional laser profilers, such as circular texture meters (CTMs) [121] and vehicle-mounted laser profilers, can capture only the profile of a single cross section and fail to obtain 3D spatial texture features.

3D laser scanners can be categorized into handheld and mobile types. Handheld scanners [122], such as the HandySCAN3D from CREAMFROM [123], are more convenient and portable but are not specifically designed for pavement, requiring a high level of human involvement. Mobile scanners acquire data through the relative motion of a camera and laser emitter. In 2011, Wang et al. [124] assembled a set of outdoor 3D laser scanning equipment, but it remained in the testing phase and was not industrialized. In recent years, manufacturers in Europe and America have encapsulated 3D cameras and lasers and implemented mechanical transmission through motors, such as the LS-40 from HyMIT in the US and the Texture Scanner series from AMES in the US, achieving industrialization of 3D laser scanning equipment [125]. These products can meet field test requirements, but their portability is limited. To address this problem, Zhang et al. installed a scanner on a movable cart. In 2022, Yang et al. [126] installed the equipment on a vehicle, achieving data collection at speeds of up to 64 km/h, with a data resolution of up to 0.1 mm.

The laser scanning method presents several advantages, including its high efficiency, consistency, repeatability, and precision, rendering it the foremost technique for data collection [127].

The advantages and limitations of the data acquisition methods for pavement textures are listed in Table 3. In conclusion, various methods and equipment are available, and the development trend is toward high precision, low cost, high efficiency, and automation. Although existing equipment may not fully meet all requirements, there are already applicable solutions for specific scenarios. The accuracy and quantity have significantly improved, providing a solid foundation for the extraction of pavement texture features and the estimation of skid resistance performance.

5.2 Feature extraction

Owing to the complexity and disorderliness of the spatial distribution of pavement texture, accurate characterization via mathematical methods is challenging. Therefore, feature extraction methods are needed to quantify and describe its spatial morphology and structural characteristics. Existing feature extraction methods mainly include mathematical geometric methods, signal processing methods, and digital image methods.

5.2.1 Mathematical geometric methods

Mathematical geometric methods can calculate parameters related to the geometric or statistical features of the pavement texture. Initially, these methods were aimed at 2D texture profiles. In 2005, Ergun et al. [37] proposed six mathematical statistical texture indices and established empirical formulas for the friction coefficient. Subsequently, an increasing number of mathematical geometric parameters have been proposed, gradually extending from 2D to 3D features [128, 129]. Pavement texture parameters can be classified as contour parameters [37], height parameters [122], functional parameters [130], volume parameters [131], and composite parameters [131].

The fractal dimension, a concept from geometric theory, has also been applied to feature extraction. Ran et al. [132] employed an improved cube covering method to calculate the 3D fractal dimension of the pavement texture. Liu et al. [133] calculated the fractal dimension of pavement texture via the differential box-counting method and studied its relationship with skid resistance. However, Miao et al. [134] have noted that using a single fractal dimension may not adequately capture the detailed features. Even with the same fractal dimension, there may be differences in local features. Therefore, fractal theory has evolved to include research on segmented dimensional variations and multifractals. Xiao et al. [135] utilized multifractal differentiation to characterize both macro- and micro-texture properties.

Mathematical geometric parameters of the pavement texture have the advantages of simplicity in calculation and ease of generalization. However, they may not fully describe the details of texture morphology at different scales.

5.2.2 Signal processing methods

In recent years, signal processing methods have been widely applied to road surface texture features, with the most representative methods being the Fourier transform, wavelet transform, and Hilbert–Huang transform [136].

The Fourier transform converts spatial domain data into the frequency domain, displaying the distribution of signals with different wavelengths through forms such as power spectral density [137]. Deng et al. [138] extracted texture features from power spectra at eight wavelengths of pavement and predicted the pavement friction coefficient, determining the optimal wavelength. However, frequency domain analysis completely obscures the spatial information of the pavement texture.

Wavelet transformation performs frequency domain analysis while preserving spatial information and separates the characteristics of the signal at different scales [139]. In 2013, Zelelew et al. [140] proposed an evaluation index for pavement profiles that is based on wavelet decomposition. Subsequently, Yang et al. [141] employed wavelet transformation to extract indices of texture profiles and established a skid resistance prediction model. Furthermore, Yang et al. [142] used discrete wavelet transformation to decompose 3D texture data into sub-images, correlating texture energy matrices of different wavelengths with measured friction data. Du et al. [143] proposed a 2D wavelet decomposition method for multi-scale feature interpretation and validated the effectiveness of this method through a comparison of the particle size distributions of different gradation types [144].

Compared with the wavelet transform, the Hilbert–Huang transform overcomes the issue of nonadaptivity of basis functions. In 2015, Kane et al. [145] used empirical mode decomposition (EMD) to analyze the pavement texture and analyzed the contribution of different wavelengths to friction, finding that small-scale and large-scale textures play dominant roles at low and high speeds, respectively [146]. Yu et al. [147] utilized the Hilbert–Huang transform to extract the amplitude and instantaneous frequency of profiles as parameters. Chen et al. [148] computed eight parameters of optimal intrinsic mode functions (OIMFs) on the basis of the Hilbert–Huang transform and explored their correlation with friction. The results revealed

Table 3 Methods for assessing pavement texture

Method	Category		Representative	Image	Advantage	Disadvantage
Probe test	Contact probes		T8000 contact probe		(1) **Precision**: high (2) **Resolution**: high	(1) **Applicability**: only suitable for laboratory scenarios (2) **Range**: limited (3) **Availability**: low (4) **Cost**: expensive (5) **Efficiency**: low (6) **Risk**: the probe may damage the texture
Laser scanners	2D	Portable	CTM	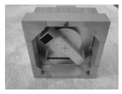	(1) **Applicability**: apply for indoor and on-site scenarios (2) **Availability**: convenient to use (3) **Cost**: low	(1) **Precision**: low (2) **Resolution**: low (3) **Range**: limited (4) **Efficiency**: low
		Vehicle-mounted	Laser profilers		(1) **Range**: wide (2) **Efficiency**: high	(1) **Precision**: low (2) **Resolution**: low (3) **Cost**: low
	3D	Handheld	HandySCAN 3D		(1) **Applicability**: apply for indoor and on-site scenarios (2) **Availability**: convenient to use	(1) **Cost**: expensive (2) **Efficiency**: low
		Portable	Texture scanner		(1) **Precision**: high (2) **Resolution**: high (3) **Applicability**: apply for indoor and on-site scenarios (4) **Availability**: convenient to use	(1) **Range**: limited (2) **Cost**: expensive
			Portable texture scanner		(1) **Precision**: high. (2) **Resolution**: high (3) **Applicability**: apply for indoor and on-site scenarios (4) **Availability**: convenient to use (5) **Efficiency**: high	(1) **Range**: limited (2) **Cost**: expensive
			Safety sensor		(1) **Resolution**: high (2) **Availability**: convenient to use (3) **Efficiency**: high	(1) **Precision**: limited (2) **Cost**: expensive
Image-based method	Monocular		Camera		(1) **Availability**: convenient to use (2) **Cost**: low (3) **Efficiency**: high	(1) **Precision**: limited
	Binocular		Binocular camera		(1) **Availability**: convenient to use (2) **Cost**: low (3) **Efficiency**: high	(1) **Precision**: limited
	Multiocular		CRP		(1) **Precision**: high (2) **Cost**: low	(1) **Applicability**: only for a laboratory scenario (2) **Range**: limited

that the parameter representing the ratio of peak density to sharpness in the OIMF had the strongest correlation with friction ($R^2 = 0.78$).

While texture features based on signal processing methods may not be intuitive, they can extract multiscale features, which are crucial for studying the contribution of textures at different scales to pavement skid resistance.

5.2.3 Digital image methods

Owing to the similarity between 3D pavement data and grayscale images, many traditional digital image processing methods, such as grayscale thresholding [149], watershed algorithms [150], morphological methods [151], edge detection [100], structural similarity [152], and image segmentation [117], have been employed for feature extraction. However, these methods are highly sensitive to edge information in images, whereas edge information in road texture data is not prominent. Therefore, these methods are more commonly applied to analyze macroscopic texture-related properties, such as texture depth, gradation type, segregation, and pavement diseases [153]. Nevertheless, their application in predicting pavement skid resistance remains limited.

The gray-level co-occurrence matrix (GLCM) [154] can effectively extract complex information from road textures and consider spatial relationships between pixels. Miao et al. [155] utilized the GLCM to extract texture features and investigated the differences in GLCM indicators under various spatial relationships between pixel pairs. Dong et al. [156] proposed evaluation indicators for pavement texture at the macroscopic and microscopic levels based on GLCM.

With the advancement of deep learning, researchers have found that convolutional neural networks (CNNs) can capture complex texture features that traditional image-processing methods cannot obtain. Therefore, in recent years, CNNs have attracted widespread attention and application in the field of pavement texture extraction. Du et al. [118] proposed a multi-feature fusion neural network for friction prediction, which uses image-processing methods, GCLM, and CNN as feature extractors.

In summary, various texture extraction methods have been proposed in existing research, each with its own advantages and limitations. However, how to effectively integrate multiple types of features to improve the prediction model of pavement skid resistance still requires further exploration.

5.3 Prediction models

With the growth of the accuracy and efficiency of 3D pavement data acquisition, many researchers have attempted to utilize machine learning methods to establish the relationship between 3D pavement data and skid resistance. These methods can be divided into two main categories: machine learning and deep neural network models. The most selected features and models are shown in Fig. 10.

5.3.1 Machine learning models

Machine learning models are mainly multivariate regression models that are based on texture feature parameters. Li et al. [157] employed a linear regression model to estimate the skid resistance on the basis of surface and aggregate texture characteristics. Chen et al. [158] utilized a multivariate nonlinear regression model for friction prediction using macro- and micro-texture features. Since 2020, many studies have employed nonlinear machine learning models for estimation. Zhan et al. [159] implemented an XGBoost architecture to allocate weights for multiple weak learners and predict BPNs on the basis of multidimensional texture features. Hu et al. [160] employed the Hyperopt-NGBoost method for skid resistance estimation. Yang et al. [161] explored the contribution of geometric parameters to friction prediction model estimation via the random forest algorithm. The macro- and micro-texture parameters account for 48.8% and 39.6% of the contribution to high-speed friction, respectively, and 50.0% and 14.1% of the contribution to low-speed friction, respectively. Zou et al. [162] obtained macro- and micro-texture features through Fourier transformation and Butterworth filtering, respectively, and predicted the SFC measured by SCRIM using a BP neural network. Hu et al. [163] proposed a friction coefficient prediction model based on improved gray wolf optimization and natural gradient boosting, where the improved gray wolf optimization algorithm was used to adjust the hyperparameters of natural gradient boosting to optimize the model structure.

Considering that not all pavement textures come into contact with rubber, researchers have proposed the concept of an effective frictional area. Du et al. [164] extracted road texture data at different proportions and calculated their corresponding three-dimensional texture characteristics. They used a machine learning model to predict BPNs, and the results showed that the prediction performance was best when the top 20% of road texture data were extracted. Ding et al. [165] compared the correlation between surface area at different depths and the BPN and reported that the surface area of road texture at a distance of 2 mm from the top exhibited the highest correlation with the BPN.

5.3.2 Deep neural network models

Currently, CNNs are most commonly used among neural network models with 3D pavement data as input. Yang et al. [166] transformed texture contours into spectrograms and used CNNs to predict friction coefficients. Tong et al. [167] employed CNNs to estimate pavement texture depth, indirectly evaluating skid resistance. Valikhani et al. [149] used data augmentation and transfer learning to predict pavement texture roughness. Zhan et al. [168] converted pavement profiles into 2D spectra and trained ResNet on 33,600 sets of data collected from multiple road types in 12 states in the US for friction prediction. Lu et al. [169] used CNNs to estimate the BPN, effectively controlling the relative error within 14%. They also investigated the influence of different contact area ratios on the estimation results and reported that using inputs with 60% texture yielded the best performance. Xu et al. [170] employed a CNN based on the InceptionV4 module to classify the skid resistance levels. Liu et al. [171] proposed a multi-input fusion network with deep aggregation modules for pavement friction estimation via subimages decomposed by 2D wavelets, with an average prediction error of 0.0935. Shi et al.

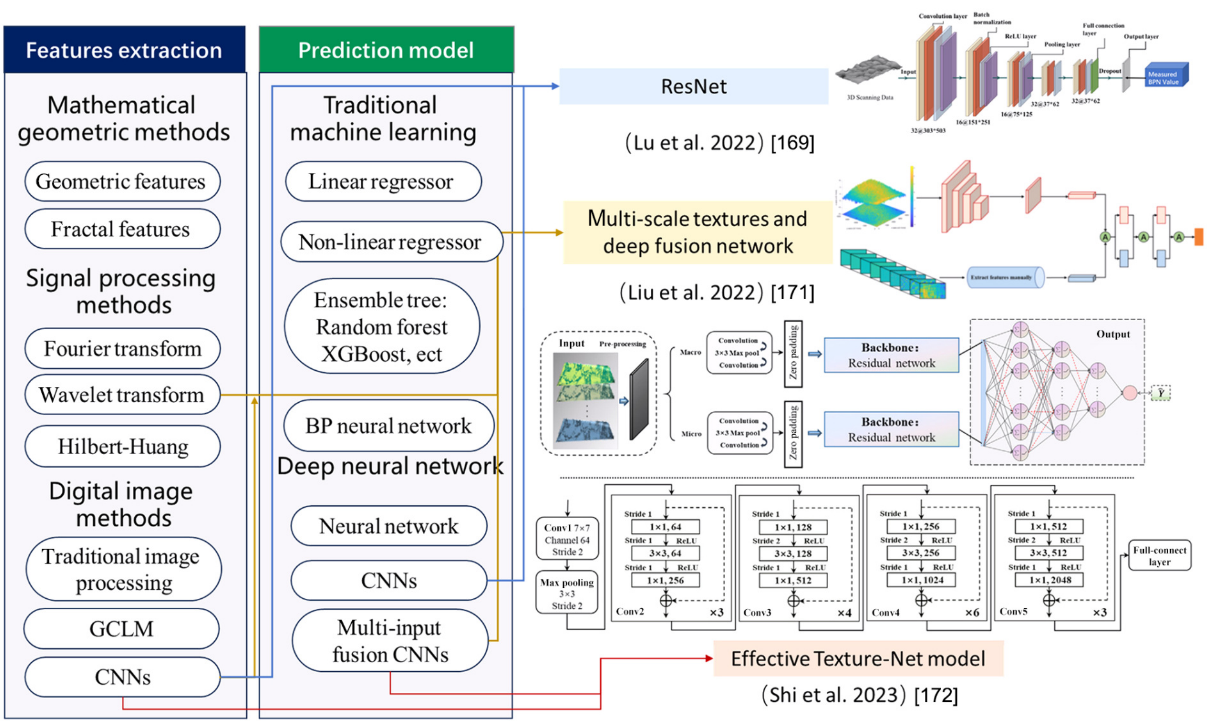

Fig. 10 Feature extraction and prediction models for various data-based models. Reproduced with permission from Ref. [169], © Elsevier Ltd. 2021; from Ref. [171], © Computer-Aided Civil and Infrastructure Engineering 2022; from Ref. [172], © Computer-Aided Civil and Infrastructure Engineering 2023.

[172] proposed an effective Texture-Net CNN model based on the contact texture area, which includes macro- and micro-scale perception sub-modules. The study revealed a significant positive correlation between the effective contact ratio parameter and the pavement skid resistance (R^2 = 0.8129), which was also influenced by the proportion of aggregates within the size range of 2.36–4.75 mm.

At present, most data-based models for predicting pavement skid resistance use extracted complex texture morphology features [173] or 3D pavement data as inputs. Deep neural network models, CNNs in particular, remain black boxes in terms of their end-to-end nature, which lack interpretability. Furthermore, their integration with the mechanics of pavement friction is relatively limited.

In conclusion, with the accumulation of data, data-based research has gradually become the primary research paradigm for evaluating pavement skid resistance. However, the integration of data with theoretical research remains a question that requires further exploration. Leveraging theory to enhance the predictive capabilities of data models and utilizing data mining to reveal the underlying mechanisms and patterns of pavement skid resistance are areas that warrant deeper investigation.

6 Challenges and future trends

Although the measurement, modeling, simulation, and estimation of pavement skid resistance have developed greatly in recent years, there is still a long way to go in terms of theoretical understanding and large-scale applications.

Currently, various pavement skid resistance measurement devices exhibit differences in principles, methods, and conditions. The correlation between their indicators is not significant enough. Consequently, the comparability of the results from different devices is weak. On the other hand, for the same devices, it is difficult to strictly control standard conditions, leading to data variability and limited applicability of the tests. This variability hampers the validation of theoretical, simulation, and data-driven research within this field, rendering their effectiveness unconvincing.

Tire–road simulation studies are often limited to specific scenarios, conditions, environments, and boundaries, making comparisons between different studies challenging. Additionally, the tire–road friction system spans from microscopic interface friction to macroscopic vehicle dynamics, yet some studies use rubber/tire simulations to assess vehicle braking risk, which is logically unsound. Simulations across different scales remain largely independent and unconnected.

In the current research on predicting pavement skid resistance on the basis of data models, pavement texture features or 3D pavement data itself are mostly used as inputs for the model. These predictive models are limited in their ability to integrate friction mechanisms [174], resulting in relatively low interpretability.

To address these problems, future development directions are elaborated.

(1) Standardized and comparable measurements for pavement skid resistance

There is an urgent need to develop widely recognized, standardized, highly repeatable, and comparable pavement skid resistance measurement methods, equipment, and indicators, especially in high-speed scenarios. These models should be applicable for field measurements and for validating various predictive models. Establishing such measurements and standards would provide a foundational benchmark for research in this field.

(2) Multimodal-driven revelation of tire–road friction mechanisms

Research on tire–road friction mechanisms is still lacking. A potential breakthrough may lie in the integration of high-resolution pavement texture features and data-driven models. These approaches can assist in revealing the mechanisms of tire–road friction and enhance the expressiveness of tire–road friction models.

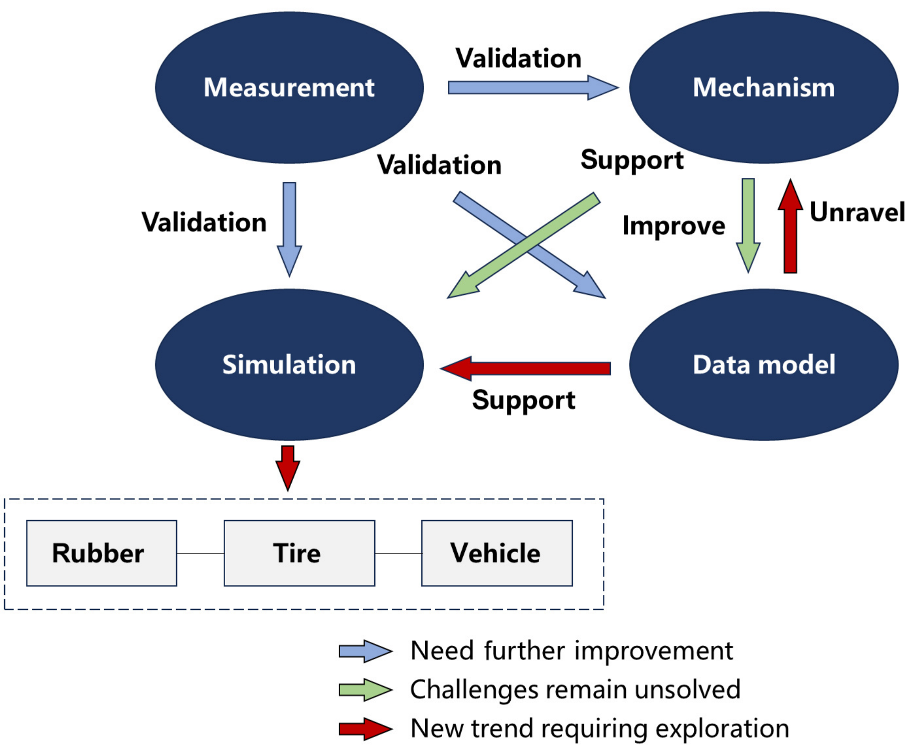

Fig. 11 Synergistic development of four research paradigms.

(3) Multiscale coupled simulation of rubber–tire–vehicle systems

The simulation offers a feasible path to achieve multiscale coupling of rubber, tire, and vehicle systems. Therefore, an important future research direction is to realize integrated simulations across these scales. This involves incorporating the friction and texture mechanisms at the rubber scale and the various factors at the tire scale into the overall vehicle braking risk assessment.

(4) Integration of data models and friction mechanisms

Integrating theoretical mechanisms with data models is an important future research direction, enhancing both the interpretability and predictive accuracy of the models.

In summary, the synergistic development of the four research paradigms can promote and advance the understanding and application of tire–road friction mechanisms, as shown in Fig. 11.

7 Concluding remarks

The tire–road friction research has been conducted for more than half a century. Understanding the tire–road friction system is fundamental for evaluating and enhancing the skid resistance of asphalt pavements. This article presents a comprehensive overview of the research paradigms and scales of asphalt pavement skid resistance evaluation. The principal summarizations are as follows.

(1) According to the literature analysis results from VOSviewer, the trajectory of tire–road friction research aligns with the evolution of scientific research paradigms: experimental science, theoretical science, computational science, and data science. Research in this field is divided into three scales: the rubber–pavement scale, the tire–road scale, and the vehicle scale.

(2) Although numerical measurement devices have been utilized for decades, the reproducibility and comparability of the results have been limited. Further enhancements are necessary for standardized highly repeatable and comparable measurement methods, equipment, and indicators. Experimental observations have revealed numerous patterns and empirical models, which form the cornerstone of this research field.

(3) The tire–road friction theory developed relatively early, but progress has slowed in recent years. Theoretical models often involve excessive simplifications, and empirical formulas are limited by various factors, but provide a theoretical foundation for tire simulation modeling.

(4) Tire–road friction simulations have been well developed across three scales, but these scales remain largely independent and unconnected.

(5) With the advancement of sensing technology, texture features have been widely exploited and used as inputs for various machine learning models to estimate pavement skid resistance. The studies were conducted in three steps: data acquisition, feature extraction, and model prediction. However, these models are limited in their ability to integrate friction mechanisms, resulting in relatively low interpretability.

Acknowledgements

This study was supported by the National Natural Science Foundation of China (Nos. 52372305, 52472327, and 52502395), the Shanghai Science and Technology Innovation Action Plan (No. 23QB1404900), and the Carbon Neutrality Funding Scheme of PolyU (No. 1-WZ7P).

Declaration of competing interest

The authors have no competing interests to declare that are relevant to the content of this article.

References

[1] Bond R, Lees G, Williams A R. An approach towards the understanding and design of the pavement's textural characteristics required for optimum performance of the tyre. In: *The Physics of Tire Traction: Theory and Experiment*. Hays D F, Browne A L, Eds. New York: Springer, 1974: 339–360.

[2] Hall J W, Smith K L, Titus-Glover L, Wambold J C, Yager T J, Rado Z. Guide for pavement friction. Washington (USA): Transportation Research Board, 2009.

[3] Khaleghian S, Emami A, Taheri S. A technical survey on tire–road friction estimation. *Friction* **5**(2): 123–146 (2017)

[4] Moore D F. *The Friction of Pneumatic Tyres*. Amsterdam (the Netherlands): Elsevier, 1975.

[5] Kogbara R B, Masad E A, Kassem E, Scarpas A (T), Anupam K. A state-of-the-art review of parameters influencing measurement and modeling of skid resistance of asphalt pavements. *Constr Build Mater* **114**: 602–617 (2016)

[6] He Y L, Cui Z B, Yang X, Wang C H, Cui K J, Fan Z P, Lu G Y, Lv S T, Wang D W. Investigating intrinsic factors in pavement skid resistance deterioration using an integrated tribology model. *Tribol Int* **199**: 109997 (2024)

[7] He Y L, Fan Z P, Yang X, Wang D W, Zhao Z J, Lu G Y, Lv S T. Study on the influence of tire polishing on surface texture durability and skid resistance deterioration of asphalt pavement. *Wear* **556–557**: 205518 (2024)

[8] van Eck N J, Waltman L. Software survey: VOSviewer, a computer program for bibliometric mapping. *Scientometrics* **84**(2): 523–538 (2010)

[9] Kuhn T S. *The Structure of Scientific Revolutions*. University of Chicago Press, 1962.

[10] Zheng B S, Chen J Y, Zhao R M, Tang J Y, Tian R Y, Zhu S Z, Huang X M. Analysis of contact behaviour on patterned tire-asphalt pavement with 3-D FEM contact model. *Int J Pavement Eng* **23**(2): 171–186 (2020)

[11] Liu X Y, Luo H Y, Chen C, Zhu L Y, Chen S Y, Ma T, Huang X M. A technical survey on mechanism and influence factors for asphalt pavement skid-resistance. *Friction* **12**(5): 845–868 (2024)

[12] Yu M, You Z P, Wu G X, Kong L Y, Liu C C, Gao J F. Measurement and modeling of skid resistance of asphalt pavement: A review. *Constr Build Mater* **260**: 119878 (2020)

[13] Jackson N M, Choubane B, Holzschuher C. Assessment of precision of circular track meter and dynamic friction tester. *Transport Res Rec* **2093**(1): 118–127 (2009)

[14] Ueckermann A, Wang D W, Oeser M, Steinauer B. Calculation of skid resistance from texture measurements. *J Traffic Transp Eng* **2**(1): 3–16 (2015)

[15] Kouchaki S, Roshani H, Prozzi J A, Garcia N Z, Hernandez J B. Field investigation of relationship between pavement surface texture and friction. *Transport Res Rec* **2672**(40): 395–407 (2018)

[16] Novikov I, Lazarev D. Experimental installation for calculation of road adhesion coefficient of locked car wheel. *Transp Res Proc* **20**: 463–467 (2017)

[17] Zuniga-Garcia N, Prozzi J A. High-definition field texture measurements for predicting pavement friction. *Transport Res Rec* **2673**(1): 246–260 (2019)

[18] Yun D, Hu L Q, Tang C. Tire–road contact area on asphalt concrete pavement and its relationship with the skid resistance. *Materials* **13**(3): 615 (2020)

[19] Han S, Liu M M, Fwa T F. Testing for low-speed skid resistance of road pavements. *Road Mater Pavement* **21**(5): 1312–1325 (2020)

[20] Zhang X D, Göhlich D. A hierarchical estimator development for estimation of tire–road friction coefficient. *PLoS One* **12**(2): e0171085 (2017)

[21] Ren H B, Chen S Z, Shim T, Wu Z C. Effective assessment of tyre–road friction coefficient using a hybrid estimator. *Vehicle Syst Dyn* **52**(8): 1047–1065 (2014)

[22] Wang Y, Hu J Y, Wang F A, Dong H X, Yan Y J, Ren Y J, Zhou C B,

Yin G D. Tire road friction coefficient estimation: Review and research perspectives. *Chin J Mech Eng* **35**(1): 6 (2022)

[23] Kumar A, Tang T C, Gupta A, Anupam K. A state-of-the-art review of measurement and modelling of skid resistance: The perspective of developing nation. *Case Stud Constr Mat* **18**: e02126 (2023)

[24] Aldagari S, Al-Assi M, Kassem E, Chowdhury A, Masad E. Development of predictive models for skid resistance of asphalt pavements and seal coat. *Int J Pavement Eng* **23**(3): 695–707 (2022)

[25] Henry J J. Evaluation of pavement friction characteristics. Washington (USA): Transportation Research Board, 2000.

[26] Quiros S B, Flintsch G W, de León Izeppi E, McGhee K K. Interconversion of locked-wheel and continuous friction measurement equipment (CFME) friction measurements. *Transport Res Rec* **2672**(40): 452–462 (2018)

[27] Flintsch G W, de León Izeppi E, McGhee K K, Roa J A. Evaluation of international friction index coefficients for various devices. *Transport Res Rec* **2094**(1): 136–143 (2009)

[28] Moyer R. A. *Skidding Characteristics of Automobile Tires on Roadway Surfaces and Their Relation to Highway Safety*. Ames (USA): Iowa State College, 1934.

[29] Leu M C, Henry J J. Prediction of skid resistance as a function of speed from pavement texture measurements. *Transport Res Rec* **666**(2): 7–13 (1978)

[30] Pillai P S, Fielding-Russell G S. Empirical equations for tire footprint area. *Rubber Chem Technol* **59**(1): 155–159 (1986)

[31] Marshek K M, Chen H H, Connell R B, Hudson W R. Experimental determination of pressure distribution of truck tire–pavement contact. *Transport Res Rec* **1070**: 9–14 (1986)

[32] Koehne S H, Matute B, Mundl R. Evaluation of tire tread and body interactions in the contact patch. *Tire Sci Technol* **31**(3): 159–172 (2003)

[33] Zhang X N, Liu T, Liu C L, Chen Z Q. Research on skid resistance of asphalt pavement based on three-dimensional laser-scanning technology and pressure-sensitive film. *Constr Build Mater* **69**: 49–59 (2014)

[34] Wang D, Ueckermann A, Schacht A, Oeser M, Steinauer B, Persson B N J. Tire–road contact stiffness. *Tribol Lett* **56**(2): 397–402 (2014)

[35] Yun D, Sha A M, Hu L Q, Tang C, Gao J. Laboratory study on the relationship between pavement texture and tread rubber penetration depth. *Int J Pavement Eng* **23**(5): 1645–1658 (2022)

[36] Meegoda J N. Non-contact skid resistance measurement. Newark (USA): New Jersey Institute of Technology, 2009.

[37] Ergun M, Iyinam S, Iyinam A F. Prediction of road surface friction coefficient using only macro- and microtexture measurements. *J Transp Eng* **131**(4): 311–319 (2005)

[38] Wu Z, King B, Abadie C, Zhang Z J. Development of design procedure to predict asphalt pavement skid resistance. *Transport Res Rec* **2306**(1): 161–170 (2012)

[39] Wasilewska M, Gardziejczyk W, Gierasimiuk P. Evaluation of skid resistance of exposed aggregate concrete pavement in the initial exploitation period. *Roads Bridges* **16**(4): 295–308 (2017)

[40] Horne W B. Wet runways. NASA Technical Memorandum, NASA-TM-X-72650, Apr. 1975.

[41] Wray G A, Ehrlich I R. A systematic experimental investigation of significant parameters affecting model tire hydroplaning. NASA-CR-132346, Jul. 1973.

[42] Wies B, Roeger B, Mundl R. Influence of pattern void on hydroplaning and related target Conflicts[4]. *Tire Sci Technol* **37**(3): 187–206 (2009)

[43] Do M T, Cerezo V, Beautru Y, Kane M. Modeling of the connection road surface microtexture/water depth/friction. *Wear* **302**(1–2): 1426–1435 (2013)

[44] Grosch K A. The relation between the friction and visco-elastic properties of rubber. *P Roy Soc Lond A Mat* **274**(1356): 21–39 (1963)

[45] Cairney P. Skid resistance and crashes: A review of the literature. Melbourne (Australia): ARRP, 1997.

[46] Khoudeir M, Brochard J, Legeay V, Do M T. Roughness characterization through 3D textured image analysis: Contribution to the study of road wear level. *Comput-Aided Civ Inf* **19**(2): 93–104 (2004)

[47] He Y L, Yang X, Xiao S Q, Liu P F, Lu G Y, Xing C, Fan Z P, Sheng W, Wang D W. Experimental study on the high-speed frictional behavior between the tire and asphalt pavement. *Constr Build Mater* **371**: 130782 (2023)

[48] PIARC. Surface characteristics. In: Proceedings of the XVIII World Road Congress, 1987.

[49] Svendenius J, Gäfvert M, Bruzelius F, Hultén J. Experimental validation of the brush tire Model. *Tire Sci Technol* **37**(2): 122–137 (2009)

[50] Canudas de Wit C, Olsson H, Astrom K J, Lischinsky P. A new model for control of systems with friction. *IEEE Automat Contr* **40**(3): 419–425 (1995)

[51] Do M T, Delanne Y. Prediction of tire/wet road friction and its variation with speed from road macro- and microtexture, and tire-related properties. In: Proceedings of the SIIV Congress on New Technologies and Modeling Tools for Roads—Applications to Design and Management, 2004.

[52] Persson B N J. Theory of rubber friction and contact mechanics. *J Chem Phys* **115**(8): 3840–3861 (2001)

[53] Persson B N J, Tartaglino U, Albohr O, Tosatti E. Sealing is at the origin of rubber slipping on wet roads. *Nat Mater* **3**(12): 882–885 (2004)

[54] Persson B N J, Tartaglino U, Albohr O, Tosatti E. Rubber friction on wet and dry road surfaces: The sealing effect. *Phys Rev B* **71**(3): 035428 (2005)

[55] Persson B N J. Rubber friction: Role of the flash temperature. *J Phys-Condens Mat* **18**(32): 7789 (2006)

[56] Persson B N J. Ice friction: Role of non-uniform frictional heating and ice premelting. *J Chem Phys* **143**(22): 224701 (2015)

[57] Klüppel M, Heinrich G. Rubber friction on self-affine road tracks. *Rubber Chem Technol* **73**(4): 578–606 (2000)

[58] Tanaka H, Yoshimura K, Sekoguchi R, Aramaki J, Hatano A, Izumi S, Sakai S, Kadowaki H. Prediction of the friction coefficient of filled rubber sliding on dry and wet surfaces with self-affine large roughness. *Mech Eng J* **3**(1): 15–00084 (2016)

[59] Ueckermann A, Wang D W, Oeser M, Steinauer B. A contribution to non-contact skid resistance measurement. *Int J Pavement Eng* **16**(7): 646–659 (2015)

[60] Motamedi M. Road surface measurement and multi-scale modeling of rubber road contact and adhesion. Ph.D. Thesis. Blacksburg (USA): Virginia Polytechnic Institute and State University, 2015.

[61] Tan T, Xing C, Tan Y Q, Gong X B. Safety aspects on icy asphalt pavement in cold region through field investigations. *Cold Reg Sci Technol* **161**: 21–31 (2019)

[62] Lorenz B, Oh Y R, Nam S K, Jeon S H, Persson B N J. Rubber friction on road surfaces: Experiment and theory for low sliding speeds. *J Chem Phys* **142**(19): 194701 (2015)

[63] Xu N, Yang Y Y, Guo K H. A discrete tire model for cornering properties considering rubber friction. *Automotive Innov* **3**(2): 133–146 (2020)

[64] Ciavarella M. A simplified version of Persson's multiscale theory for rubber friction due to viscoelastic losses. *J Tribol* **140**: 011403 (2018)

[65] Alhasan A, Smadi O, Bou-Saab G, Hernandez N, Cochran E. Pavement friction modeling using texture measurements and pendulum skid tester. *Transport Res Rec* **2672**(40): 440–451 (2018)

[66] Persson B N J. Surface roughness-induced stress concentration. *Tribol Lett* **71**(2): 66 (2023)

[67] Kane M, Cerezo V. A contribution to tire/road friction modeling: From a simplified dynamic frictional contact model to a "Dynamic Friction Tester" model. *Wear* **342–343**(3): 163–171 (2015)

[68] Kane M, Do M T, Cerezo V, Rado Z, Khelifi C. Contribution to pavement friction modelling: An introduction of the wetting effect. *Int J Pavement Eng* **20**(8): 965–976 (2019)

[69] Löwer J, Wagner P, Unrau H J, Bederna C, Gauterin F. Physical model of tire–road contact under wet conditions. *Tribol Lett* **68**(1): 25 (2020)

[70] Svendenius J. Tire modeling and friction estimation. Ph.D. Thesis. Lund (Sweden): Lund University, 2007.

[71] Gim G, Nikravesh P E. A three dimensional tire model for steady-state simulations of vehicles. *SAE Transactions* **102**: 150–159 (1993)
[72] Bakker E, Pacejka H B, Lidner L. A new tire model with an application in vehicle dynamics studies. *SAE Transactions* **98**: 101–113 (1989)
[73] Guo K H, Lu D, Chen S K, Lin W C, Lu X P. The UniTire model: A nonlinear and non-steady-state tyre model for vehicle dynamics simulation. *Vehicle Syst Dyn* **43**(sup1): 341–358 (2005)
[74] Hertz H. On the contact of elastic solids. *J Reine Angew Math* **92**: 156–171 (1882)
[75] Archard J F. Elastic deformation and the laws of friction. *P Roy Soc Lond A Mat* **243**(1233): 190–205 (1957)
[76] Greenwood J A, Williamson J B P. Contact of nominally flat surfaces. *P Roy Soc Lond A Mat* **295**(1442): 300–319 (1966)
[77] Sayles R S, Thomas T R. The spatial representation of surface roughness by means of the structure function: A practical alternative to correlation. *Wear* **42**(2): 263–276 (1977)
[78] Majumdar A, Bhushan B. Fractal model of elastic-plastic contact between rough surfaces. *J Tribol* **113**(1): 1–11 (1991)
[79] Canudas de Wit C, Tsiotras P, Velenis E, Basset M, Gissinger G. Dynamic friction models for road/tire longitudinal interaction. *Vehicle Syst Dyn* **39**(3): 189–226 (2003)
[80] Pinnington R J. A particle-envelope surface model for road–tyre interaction. *Int J Solids Struct* **49**(3–4): 546–555 (2012)
[81] Kane M, Edmondson V. Tire/road friction prediction: Introduction a simplified numerical tool based on contact modelling. *Vehicle Syst Dyn* **60**(3): 770–789 (2022)
[82] Lenasi J, Danon G, Žežclj S. Lateral stability of a braking vehicle on the friction limit. *Vehicle Syst Dyn* **29**(sup1): 711–716 (1998)
[83] Xu G L, Xu J L, Gao C, Sun R S, Shan H G, Ma Y J, Ran J S. A novel safety assessment framework for pavement friction evolution due to traffic on horizontal curves. *Sustainability* **14**(17): 10714 (2022)
[84] Hou Y, Wang X F, Sun W J, Wang L B. A multiscale DEM–FEM approach to investigate the tire–pavement friction. *Int J Pavement Eng* **19**(5): 399–406 (2018)
[85] Peng Y, Li J Q, Zhan Y, Wang K C P, Yang G W. Finite element method-based skid resistance simulation using *in situ* 3D pavement surface texture and friction data. *Materials* **12**(23): 3821 (2019)
[86] Guo F C, Zhang J P, Chen Z X, Zhang M L, Pei J Z, Li R. Investigation of friction behavior between tire and pavement by molecular dynamics simulations. *Constr Build Mater* **300**: 124037 (2021)
[87] Xiao M M, Cheng W. Mechanism analysis of anti-skid performance attenuation of wet pavement based on micro-interface. *Int J Pavement Res T* **17**(5): 1180–1192 (2024)
[88] Löwer J, Wagner P, Unrau H J, Wies B, Gauterin F. Model for the pattern-dependent wet grip prediction of tires. *Vehicles* **3**(1): 84–110 (2021)
[89] Tielking J T, Roberts F L. Tire contact pressure and its effect on pavement strain. *J Transp Eng* **113**(1): 56–71 (1987)
[90] Burke A M, Olatunbosun O A. Static tyre/road interaction modelling. *Meccanica* **32**(5): 473–479 (1997)
[91] Wei S, Wang Y H, Cheng H L, Wang D W. Stress distributions in the textures of prefabricated pavement surface created with the assistance of 3D printing technology. *Int J Pavement Eng* **24**(1): 2005058 (2021)
[92] Li Z, Chen W Y, Li Y H, Wu W L. Finite element analysis of tyre contact interaction considering simplified pavement with different aggregate sizes. *Appl Sci* **13**(21): 12011 (2023)
[93] Anupam K, Srirangam S K, Scarpas A, Kasbergen C, Kane M. Study of cornering maneuvers of a pneumatic tire on asphalt pavement surfaces using the finite element method. *Transport Res Rec* **2457**(1): 129–139 (2014)
[94] Anupam K, Srirangam S K, Scarpas A, Kasbergen C. Influence of temperature on tire–pavement friction: Analyses. *Transport Res Rec* **2369**(1): 114–124 (2013)
[95] Ong G P, Fwa T F. Wet-pavement hydroplaning risk and skid resistance: Modeling. *J Transp Eng* **133**(10): 590–598 (2007)
[96] Fwa T F, Pasindu H R, Ong G P. Critical rut depth for pavement maintenance based on vehicle skidding and hydroplaning consideration. *J Transp Eng* **138**(4): 423–429 (2012)
[97] Ding Y M, Wang H. Evaluation of hydroplaning risk on permeable friction course using tire–water–pavement interaction model. *Transport Res Rec* **2672**(40): 408–417 (2018)
[98] Choi J H, Cho J R, Woo J S, Kim K W. Numerical investigation of snow traction characteristics of 3-D patterned tire. *J Terramechanics* **49**(2): 81–93 (2012)
[99] Zhu S Z, Liu X Y, Cao Q Q, Huang X M. Numerical study of tire hydroplaning based on power spectrum of asphalt pavement and kinetic friction coefficient. *Adv Mater Sci Eng* **2017**(1): 5843061 (2017)
[100] Zhu X Y, Yang Y, Zhao H D, Jelagin D, Chen F, Gilabert F A, Guarin A. Effects of surface texture deterioration and wet surface conditions on asphalt runway skid resistance. *Tribol Int* **153**: 106589 (2021)
[101] Luo H Y, Chen S Y, Zhu L Y, Liu X Y, Zheng Y, Zhao R M, Huang X M. Investigation of surface textures deterioration on pavement skid-resistance using hysteresis friction models and numerical simulation method. *Friction* **12**(4): 745–779 (2024)
[102] Fan, Y H, Zhu, X Y, Yang, H L, Wang, L B. Analysis of effects of worn-out surface texture and wet surface on asphalt pavement skid resistance through FEM–VDM modeling. *China J Highw Transp* **36**(12): 318–332 (2023) (in Chinese)
[103] Tian G, Jia Y S, Chen Z Q, Gao Y, Wang S Q, Wei Z Y, Chen Y F, Zhang T S. Evaluation on lateral stability of vehicle: Impacts of pavement rutting, road alignment, and adverse weather. *Appl Sci* **13**(5): 3250 (2023)
[104] Liu X Y, Cao Q Q, Wang H, Chen J Y, Huang X M. Evaluation of vehicle braking performance on wet pavement surface using an integrated tire–vehicle modeling approach. *Transport Res Rec* **2673**(3): 295–307 (2019)
[105] You K S, Sun L. Reliability analysis of vehicle stability on combined horizontal and vertical alignments: Driving safety perspective. *J Transp Eng* **139**(8): 804–813 (2013)
[106] Peng J, Chu L, Fwa T F. Determination of safe vehicle speeds on wet horizontal pavement curves. *Road Mater Pavement* **22**(11): 2641–2653 (2021)
[107] Zheng B S, Huang X M, Tang J Y, Chen J Y, Zhao R M, Hong Z Q, Tang T, Han M L. Evaluation on braking stability of autonomous vehicles running along curved sections based on asphalt pavement adhesion properties. *J Adv Transport* **2022**(1): 7348554 (2022)
[108] Zhao, H D, Zhao, L R, Cai, J W, Ma, L K. Quantitative evaluation of hydroplaning risk on wet pavement based on critical hydroplaning velocity. *J Tongji Univ Nat Sci* **51**(8): 1174–1181 (2023) (in Chinese)
[109] US-ASTM. ASTM E965-96 Standard test method for measuring pavement macrotexture depth using a volumetric technique. ASTM, 1996.
[110] US-ASTM. ASTM E2380-05 Standard test method for measuring pavement texture drainage using an outflow meter. ASTM, 2005.
[111] Chu C, Wang L B, Yang H L, Tang X C, Chen Q Y. An optimized fringe generator of 3D pavement profilometry based on laser interference fringe. *Opt Lasers Eng* **136**: 106142 (2021)
[112] Du Y C, Li Y S, Jiang S C, Shen Y. Mobile light detection and ranging for automated pavement friction estimation. *Transport Res Rec* **2673**(10): 663–672 (2019)
[113] Carmon N, Ben-Dor E. Mapping asphaltic roads' skid resistance using imaging spectroscopy. *Remote Sens* **10**(3): 430 (2018)
[114] Masad E, Button J W. Unified imaging approach for measuring aggregate angularity and texture. *Comput-Aided Civ Inf* **15**(4): 273–280 (2000)
[115] Ghaderi O, Abedini M. Evaluation of the airport runway flexible pavement macro-texture using digital image processing technique (DIPT). *Int J Pavement Eng* **23**(13): 4587–4599 (2022)
[116] Nejad F M, Karimi N, Zakeri H. Automatic image acquisition with knowledge-based approach for multi-directional determination of skid resistance of pavements. *Automat Constr* **71**: 414–429 (2016)
[117] Weng Z H, Xiang H, Lin Y C, Liu C L, Wu D F, Du Y C. Pavement

texture depth estimation using image-based multiscale features. *Automat Constr* **141**: 104404 (2022)
[118] Du Y C, Liu C L, Song Y, Li Y S, Shen Y. Rapid estimation of road friction for anti-skid autonomous driving. *IEEE T Intell Transp* **21**(6): 2461–2470 (2020)
[119] Chen J Y, Huang X M, Zheng B S, Zhao R M, Liu X Y, Cao Q Q, Zhu S Z. Real-time identification system of asphalt pavement texture based on the close-range photogrammetry. *Constr Build Mater* **226**: 910–919 (2019)
[120] Sun L, Wang Y Y. Three-dimensional reconstruction of macrotexture and microtexture morphology of pavement surface using six light sources-based photometric stereo with low-rank approximation. *J Comput Civil Eng* **31**(2): 04016054 (2017)
[121] Prowell B D, Hanson D I. Evaluation of circular texture meter for measuring surface texture of pavements. *Transport Res Rec* **1929**(1): 88–96 (2005)
[122] Čelko J, Kováč M, Kotek P. Analysis of the pavement surface texture by 3D scanner. *Transp Res Proc* **14**: 2994–3003 (2016)
[123] Hu L Q, Yun D, Gao J, Tang C. Monitoring and optimizing the surface roughness of high friction exposed aggregate cement concrete in exposure process. *Constr Build Mater* **230**: 117005 (2020)
[124] Wang W F, Yan X P, Huang H L, Chu X M, Abdel-Aty M. Design and verification of a laser based device for pavement macrotexture measurement. *Transport Res C—Emer* **19**(4): 682–694 (2011)
[125] Jiang J Q, Ketabdari M, Crispino M, Toraldo E. Estimating vehicle braking distance over wet and rutted pavement surface through back-propagation neural network. *Results Eng* **21**: 101686 (2024)
[126] Yang G W, Wang K C P, Li J Q, Wang G L. A novel 0.1 mm 3D laser imaging technology for pavement safety measurement. *Sensors* **22**(20): 8038 (2022)
[127] Li L P, Li Y S, Du Y C, Liu C L, Wu D F. Digital sand patch: Using laser scanning and discrete element simulation for rapider pavement texture depth measurement. *Measurement* **236**: 115139 (2024)
[128] Wang Y Y, Yang Z Q, Liu Y Y, Sun L. The characterisation of three-dimensional texture morphology of pavement for describing pavement sliding resistance. *Road Mater Pavement* **20**(5): 1076–1095 (2019)
[129] Bitelli G, Simone A, Girardi F, Lantieri C. Laser scanning on road pavements: A new approach for characterizing surface texture. *Sensors* **12**(7): 9110–9128 (2012)
[130] Li Q J, Yang G W, Wang K C P, Zhan Y J, Wang C H. Novel macro- and microtexture indicators for pavement friction by using high-resolution three-dimensional surface data. *Transport Res Rec* **2641**(1): 164–176 (2017)
[131] Hu L Q, Yun D, Liu Z Z, Du S W, Zhang Z, Bao Y B. Effect of three-dimensional macrotexture characteristics on dynamic frictional coefficient of asphalt pavement surface. *Constr Build Mater* **126**: 720–729 (2016)
[132] Ran M P, Xiao S Q, Zhou X L, Xiao W X. Evaluation of segregation in asphalt pavement surface using concave multifractal distribution. *J Test Eval* **46**(5): 2100–2109 (2018)
[133] Liu Y, Qian Z D, Hu H B, Shi X J, Chen L L. Developing a skid resistance prediction model for newly built pavement: Application to a case study of steel bridge deck pavement. *Road Mater Pavement* **23**(10): 2334–2352 (2022)
[134] Miao Y H, Song P P, Gong X Q. Fractal and multifractal characteristics of 3D asphalt pavement macrotexture. *J Mater Civil Eng* **26**(8): 04014033 (2014)
[135] Xiao S Q, Tan Y Q, Xing C, Zhou X L. Scale demarcation of self-affine surface of coarse aggregate and its relationship with rubber friction. *Road Mater Pavement* **22**(8): 1842–1859 (2021)
[136] Ayenu-Prah A Y, Attoh-Okine N O. Comparative study of Hilbert–Huang transform, Fourier transform and wavelet transform in pavement profile analysis. *Vehicle Syst Dyn* **47**(4): 437–456 (2009)
[137] Hartikainen L, Petry F, Westermann S. Frequency-wise correlation of the power spectral density of asphalt surface roughness and tire wet friction. *Wear* **317**(1–2): 111–119 (2014)
[138] Deng Q S, Zhan Y, Liu C, Qiu Y J, Zhang A. Multiscale power spectrum analysis of 3D surface texture for prediction of asphalt pavement friction. *Constr Build Mater* **293**: 123506 (2021)
[139] Lin Y C, Dong C Y, Wu D F, Jiang S C, Xiang H, Weng Z H. Study of pavement macro- and micro-texture evolution law during compaction using 3D laser scanning technology. *Appl Sci* **13**(9): 5736 (2023)
[140] Zelelew H M, Papagiannakis A T, de León Izeppi E D. Pavement macro-texture analysis using wavelets. *Int J Pavement Eng* **14**(8): 725–735 (2013)
[141] Yang G W, Li Q J, Zhan Y J, Wang K C P, Wang C H. Wavelet based macrotexture analysis for pavement friction prediction. *KSCE J Civ Eng* **22**(1): 117–124 (2018)
[142] Yang G W, Wang K C P, Li J Q. Multiresolution analysis of three-dimensional (3D) surface texture for asphalt pavement friction estimation. *Int J Pavement Eng* **22**(14): 1882–1891 (2021)
[143] Du Y C, Weng Z H, Li F, Ablat G, Wu D F, Liu C L. A novel approach for pavement texture characterisation using 2D-wavelet decomposition. *Int J Pavement Eng* **23**(6): 1851–1866 (2022)
[144] Weng Z H, Ablat G, Wu D F, Liu C L, Li F, Du Y C, Cao J. Rapid pavement aggregate gradation estimation based on 3D data using a multi-feature fusion network. *Automat Constr* **134**: 104050 (2022)
[145] Kane M, Rado Z, Timmons A. Exploring the texture–friction relationship: From texture empirical decomposition to pavement friction. *Int J Pavement Eng* **16**(10): 919–928 (2015)
[146] Kane M, Edmondson V. Skid resistance: Understanding the role of road texture scales using a signal decomposition technique and a friction model. *Int J Pavement Eng* **23**(2): 499–513 (2022)
[147] Yu W Y, Li J Q, Yang G W, Wang K C P, Attoh-Okine N. Hilbert-Huang transformation (HHT) based texture profile analysis for continuous friction characterisation of pavements. *Int J Pavement Eng* **23**(6): 2074–2082 (2022)
[148] Chen C, Luo H Y, Chen S Y, Zheng Y, Liu X Y, Ma T, Zhu L Y. Exploring the relationship between pavement surface texture and friction based on Hilbert–Huang Transformation. *Tribol Int* **187**: 108737 (2023)
[149] Valikhani A, Jaberi Jahromi A, Pouyanfar S, Mantawy I M, Azizinamini A. Machine learning and image processing approaches for estimating concrete surface roughness using basic cameras. *Comput-Aided Civ Inf* **36**(2): 213–226 (2021)
[150] Cao R J, Zhao Y L, Gao Y, Huang X M, Zhang L L. Effects of flow rates and layer thicknesses for aggregate conveying process on the prediction accuracy of aggregate gradation by image segmentation based on machine vision. *Constr Build Mater* **222**: 566–578 (2019)
[151] Wan T T, Wang H N, Feng P N, Diab A. Concave distribution characterization of asphalt pavement surface segregation using smartphone and image processing based techniques. *Constr Build Mater* **301**: 124111 (2021)
[152] Zhang X, Wang H, Chi M, Xu Z C, Xu G C. Experimental investigation on wear behavior of asphalt pavement based on three-dimensional surface texture scan technology. *Constr Build Mater* **412**: 134851 (2024)
[153] Shi J C, Gong H R, Cong L, Liang H M, Ren M D. Evaluating and quantifying segregation in asphalt pavement construction: A state-of-the-practice survey. *Constr Build Mater* **383**: 131205 (2023)
[154] Haralick R M, Shanmugam K, Dinstein I. Textural features for image classification. *IEEE T Syst Man Cyb* **SMC-3**(6): 610–621 (1973)
[155] Miao Y H, Wang L B, Wang X F, Gong X Q. Characterizing asphalt pavement 3-D macrotexture using features of Co-occurrence matrix. *Int J Pavement Res T* **8**(4): 243–250 (2015)
[156] Dong S H, Han S, Zhang Q X, Han X, Zhang Z, Yao T F. Three-dimensional evaluation method for asphalt pavement texture characteristics. *Constr Build Mater* **287**: 122966 (2021)
[157] Li Q J, Zhan Y, Yang G W, Wang K C P. Pavement skid resistance as a function of pavement surface and aggregate texture properties. *Int J Pavement Eng* **21**(10): 1159–1169 (2020)
[158] Chen D, Han S, Ye A J, Ren X C, Wang W, Wang T T. Prediction of

tire–pavement friction based on asphalt mixture surface texture level and its distributions. *Road Mater Pavement* **21**(6): 1545–1564 (2020)
[159] Zhan Y, Liu C, Deng Q S, Feng Q, Qiu Y J, Zhang A, He X L. Integrated FFT and XGBoost framework to predict pavement skid resistance using automatic 3D texture measurement. *Measurement* **188**: 110638 (2022)
[160] Hu Y J, Sun Z Y, Han Y X, Hao X L, Pei L L. Pavement skid resistance evaluation based on hyperopt-NGBoost fusion model using non-contact measurement of 3D macrotexture data. *Arab J Sci Eng* **48**(4): 5507–5524 (2023)
[161] Yang G W, Yu W Y, Li Q J, Wang K, Peng Y, Zhang A N. Random forest-based pavement surface friction prediction using high-resolution 3D image data. *J Test Eval* **49**(2): 1141–1152 (2021)
[162] Zou Y W, Yang G W, Cao M M. Neural network-based prediction of sideway force coefficient for asphalt pavement using high-resolution 3D texture data. *Int J Pavement Eng* **23**(9): 3157–3166 (2022)
[163] Hu Y J, Sun Z Y, Pei L L, Han Y X, Li W. Evaluate asphalt pavement frictional characteristics based on IGWO-NGBoost using 3D macro-texture data. *Expert Syst Appl* **242**: 122786 (2024)
[164] Du Y C, Qin B H, Weng Z H, Wu D F, Liu C L. Promoting the pavement skid resistance estimation by extracting tire-contacted texture based on 3D surface data. *Constr Build Mater* **307**: 124729 (2021)
[165] Ding S H, Wang K C P, Yang E H, Zhan Y. Influence of effective texture depth on pavement friction based on 3D texture area. *Constr Build Mater* **287**: 123002 (2021)
[166] Yang G W, Li Q J, Zhan Y, Fei Y, Zhang A N. Convolutional neural network-based friction model using pavement texture data. *J Comput Civil Eng* **32**(6): 04018052 (2018)
[167] Tong Z, Gao J, Sha A M, Hu L Q, Li S. Convolutional neural network for asphalt pavement surface texture analysis. *Comput-Aided Civ Inf* **33**(12): 1056–1072 (2018)
[168] Zhan Y, Li J Q, Yang G W, Wang K C P, Yu W Y. Friction-ResNets: Deep residual network architecture for pavement skid resistance evaluation. *J Transp Eng B—Pave* **146**(3): 04020027 (2020)
[169] Lu J L, Pan B F, Liu Q, Sun M H, Liu P F, Oeser M. A novel noncontact method for the pavement skid resistance evaluation based on surface texture. *Tribol Int* **165**: 107311 (2022)
[170] Xu G M, Lin X Q, Wang S F, Zhan Y, Liu J, Huang H. Incep-FrictionNet-based pavement texture friction level classification prediction method. *Lubricants* **12**(1): 8 (2024)
[171] Liu C L, Xu N, Weng Z H, Li Y S, Du Y C, Cao J. Effective pavement skid resistance measurement using multi-scale textures and deep fusion network. *Comput-Aided Civ Inf* **38**(8): 1041–1058 (2023)
[172] Shi W B, Niu D Y, Li Z R, Niu Y H. Effective contact texture region aware pavement skid resistance prediction via convolutional neural network. *Comput-Aided Civ Inf* **39**(13): 2054–2070 (2024)
[173] Tan Z F, Guo F Q, Leng Z, Yang Z J, Cao P. A novel strategy for generating mesoscale asphalt concrete model with controllable aggregate morphology and packing structure. *Comput Struct* **296**: 107315 (2024)
[174] Weng Z H, Liu C L, Du Y C, Wu D F, Leng Z. Integrating spatial and channel attention mechanisms with domain knowledge in convolutional neural networks for friction coefficient prediction. *Comput-Aided Civ Inf* **40**(17): 2480–2497 (2025)

Zihang Weng received his bachelor degree in civil engineering from Tongji University, Shanghai, China, in 2018 and his Ph.D. degree in transportation engineering from Tongji University in 2024. He is currently a postdoctoral researcher in the Department of Civil and Environmental Engineering, Hong Kong Polytechnic University, Hong Kong, China. During the period from 2022 to 2023, he served as an academic guest with the Infrastructure Management Group at the Institute of Construction & Infrastructure Management at ETH Zürich, Zürich, Switzerland. His research interests lie in the field of pavement condition assessment by emerging sensing technologies.

Chenglong Liu received his B.S. and Ph.D. degrees in transportation engineering from Tongji University, Shanghai, China, in 2014 and 2019, respectively. From 2020 to 2022, he was an associate research fellow with the Transportation Research Institute, Tongji University. He is currently an associate professor with the College of Transportation Engineering, Tongji University. He is the author of more than 50 articles and more than 20 inventions. His research interests include road infrastructure management, pavement condition measurement, intelligent transportation systems, and AI techniques in transportation.

Yuchuan Du received his bachelor and master degrees in road engineering from Tongji University, Shanghai, China, in 1998 and 2001, respectively, and his Ph.D. degree in traffic engineering from Tongji University in 2004. From 2003 to 2006, he was an assistant professor at the College of Transportation Engineering at Tongji University, where he was also an associate professor at the College of Transportation Engineering from 2006 to 2010. In 2010, he was promoted to professor and the vice dean of the College of Transportation Engineering at Tongji University. His research interests include innovative technology for smart infrastructure and autonomous vehicles.

Zhen Leng received his Ph.D. degree from the University of Illinois at Urbana-Champaign, Urbana, IL, USA, in 2011. He is currently a professor of civil and environmental engineering at Hong Kong Polytechnic University, Hong Kong, China. He serves as the director of the Road Research Laboratory and the associate director of the Research Centre for Resources Engineering toward Carbon Neutrality. His research interests include sustainable infrastructure materials and technologies, eco-efficiency analysis and life cycle assessment, and nondestructive evaluation of transportation infrastructure.

Difei Wu received his bachelor and Ph.D. degrees in transportation engineering from Tongji University, Shanghai, China, in 2014 and 2019, respectively. He is currently an associate researcher at the College of Transportation Engineering, Tongji University. His research interests include emerging digitalization technology for road maintenance and management.

Bryan T. Adey obtained his doctorate degree in technical sciences in civil engineering from the Swiss Federal Institute of Technology in Lausanne, Switzerland, in 2002; his master degree of science in structural engineering from the University of Alberta, Edmonton, Canada, in 1997; and his bachelor of engineering from Dalhousie University, Halifax, Canada, in 1995. Prof. Adey's research is focused on improving the effectiveness and efficiency of infrastructure management.